THE CHARACTERISATION OF TITAN'S ATMOSPHERIC PHYSICAL PROPERTIES BY THE HUYGENS ATMOSPHERIC STRUCTURE INSTRUMENT (HASI)

M. FULCHIGNONI[1,3], F. FERRI[2,7], F. ANGRILLI[2], A. BAR-NUN[4], M.A. BARUCCI[1], G. BIANCHINI[2], W. BORUCKI[5], M. CORADINI[6], A. COUSTENIS[1], P. FALKNER[7], E. FLAMINI[8], R. GRARD[7], M. HAMELIN[9], A.M. HARRI[10], G.W. LEPPELMEIER[10], J.J. LOPEZ-MORENO[11], J.A.M. MCDONNELL[12], C.P. MCKAY[5], F.H. NEUBAUER[13], A. PEDERSEN[14], G. PICARDI[15], V. PIRRONELLO[16], R. RODRIGO[11], K.SCHWINGENSCHUH[17], A. SEIFF[18], H. SVEDHEM[7], V. VANZANI[2], J. ZARNECKI[12]

[1]*Département de Recherche Spatiale (DESPA), Obs. Paris-Meudon, France*
[2]*C.I.S.A.S. Centre of Studies and Activities for Space 'G. Colombo', Univ. Padova (UPD), Italy*
[3]*Université Denis Diderot - Paris 7, France*
[4]*Dept. Of Geophysics and Planetary Sciences, Univ. Tel Aviv, Israel*
[5]*NASA/AMES, Moffett Field CA 94035, USA*
[6]*ESA, Science Directorate, Paris, France*
[7]*ESTEC, Solar System Division (SSD), Noordwijk, The Netherlands*
[8] *Agenzia Spaziale Italiana, Roma, Italy*
[9]*Laboratoire de Physique et Chimie de l'Environnement (LPCE), Orleans, France*
[10]*Finnish Meteorological Institute (FMI), Helsinki, Finland*
[11]*Instituto de Astrofisica de Andalucia (IAA-CSIC), Granada, Spain*
[12]*University of Kent (UKC), Canterbury, UK*
[13]*University of Köln, Germany*
[14]*University of Oslo, Norway*
[15]*University 'La Sapienza', Roma, Italy*
[16]*Osservatorio Astrofisico di Catania, Italy*
[17]*Space Research Institute, Austrian Academy of Sciences (IWF), Graz, Austria*
[18]*San José State University Foundation, Dept. of Meteorology, San José, CA 95192-0104*

Received 22 December 1998; Accepted in final form 20 March 2000

Abstract. The Huygens Atmospheric Structure Instrument (HASI) is a multi-sensor package which has been designed to measure the physical quantities characterising the atmosphere of Titan during the Huygens probe descent on Titan and at the surface. HASI sensors are devoted to the study of Titan's atmospheric structure and electric properties, and to provide information on its surface, whether solid or liquid.

1. Introduction

The Huygens Atmospheric Structure Instrument (HASI) is one of the six experiments comprising the payload of the Huygens probe, which will be released by the Cassini spacecraft to descend onto Titan. During the descent and after the

Space Science Reviews **104:** 395–431, 2002.

landing, the instrumentation on board the probe will make measurements to investigate Titan's environment. HASI has been designed to measure the physical quantities characterising Titan's atmosphere, including the density, temperature, and pressure profiles, winds, turbulence and electric properties. HASI data will also contribute to the analysis of the atmospheric composition and provide information on the surface, whatever its phase: liquid or solid. HASI will monitor the acceleration experienced by the probe during the entire descent phase and will provide the only direct measurements of the ambient atmospheric pressure and temperature through sensors having access to the atmospheric flow. Electrical measurements will be performed in order to characterise the electrical environment on Titan and to detect effects connected to electrical processes, such as lightning and thunder. In situ measurements are essential for the investigation of the atmospheric structure and dynamics. Estimates of the temperature lapse rate can be combined with composition measurements to identify the presence of condensation and clouds, to distinguish between saturated and unsaturated, stable and conditionally stable regions. Variations in the density, pressure and temperature profiles constrain the atmospheric stability and stratification, thermal tides, waves and turbulence in the atmosphere. Moreover, the descent profile can be derived from temperature and pressure data as a function of pressure and altitude. The return signal of the Huygens radar altimeter is processed by the HASI electronics, providing an independent estimation of altitude and the spectral analysis of the signal yields information on the satellite's surface.

In addition the HASI in situ measurements will provide a high-resolution reference for calibration of some remote sensing observations from the orbiter and the measurements of other Huygens experiments.

HASI is a multifunction experiment package originally proposed as an international collaboration including 17 institutions from 11 countries. HASI has been funded by the Italian Space Agency (ASI) and by other European institutions that provided hardware elements. The HASI subsystems and elements have been designed, developed, and built in the different institutes and by Officine Galileo (OG), Firenze, Italy.

2. HASI Subsystems and Sensor Packages

The HASI experiment is divided into four subsystems: the accelerometers (ACC); the deployable booms system (DBS); the stem (STUB) carrying the temperature sensors, a Kiel probe pressure sampling inlet, an acoustic sensor, and the data processing unit (DPU). The HASI subsystems, their acronyms, the institutions responsible for the management (together with the providers) and the elements included are summarised in Table I.

The scientific measurements are performed by four sensor packages: the accelerometers (ACC), the temperature sensors (TEM), the Pressure Profile Instrument

TABLE I
HASI subsystems

Subsystem	Responsible Institutions (Providers)*	Elements
Deployable Boom System (DBS)	SSD (LPCE/SSD)	PWA electrodes, Boom Magnetic Actuators, PWA preamplifiers (HASI-I)
Fixed stem (STUB)	UPD (UPD/FMI/IWF)	Temperature sensors, PPI Kiel probe, acoustic sensor
Accelerometers (ACC)	UKC (UKC)	Four accelerometers
Data Processing Unit (DPU)	OG (FMI/IWF/IAA/OG)	Electronics boards
Electrical Ground Support Equipment	OG (UPD/OG)	EGSE

*Refer to the authors' affiliation for institute acronyms.

(PPI) and the Permittivity, Wave and Altimetry package (PWA) (see Table II). The block diagram of the HASI experiment is reported in Figure 1.

TEM, PWA sensors and the Kiel probe of PPI are mounted outside the Huygens probe by means of booms attached to the probe ring. The other HASI elements are placed on the probe experiment platform; see Figure 2 for HASI accommodation on the Huygens probe.

2.1. HASI SUBSYSTEMS

2.1.1. *The Accelerometer Box (ACC)*

The Accelerometer subsystem (ACC) consists of a small box ($60\times80\times70$ mm) placed at the centre of mass of the descent module of the Huygens probe (see Figure 3). The box contains four accelerometers, two temperature sensors and their conditioning electronics and is connected via a cable to the DPU where acceleration data are handled.

2.1.2. *The Deployable Boom System (DBS)*

The Deployable Boom Subsystem (DBS) consists of two units with release mechanisms, each carrying three PWA electrodes connected to two pre-amplifier boxes (HASI-I). The booms are stowed under the thermal shield during the interplanetary cruise and are released by a magnetic actuator (MCA) and deployed by a coil spring, at the beginning of the descent in Titan's atmosphere (Figure 4).

The PWA sensors on each boom consist of two rings forming the receiving and transmitting antennas of the mutual impedance experiment (RX & TX), and a disk for relaxation probe measurements (RP) (see Figure 5). The receiving and the relaxation probes are connected to the preamplifiers contained in the HASI-I boxes (Grard *et al.*, 1995).

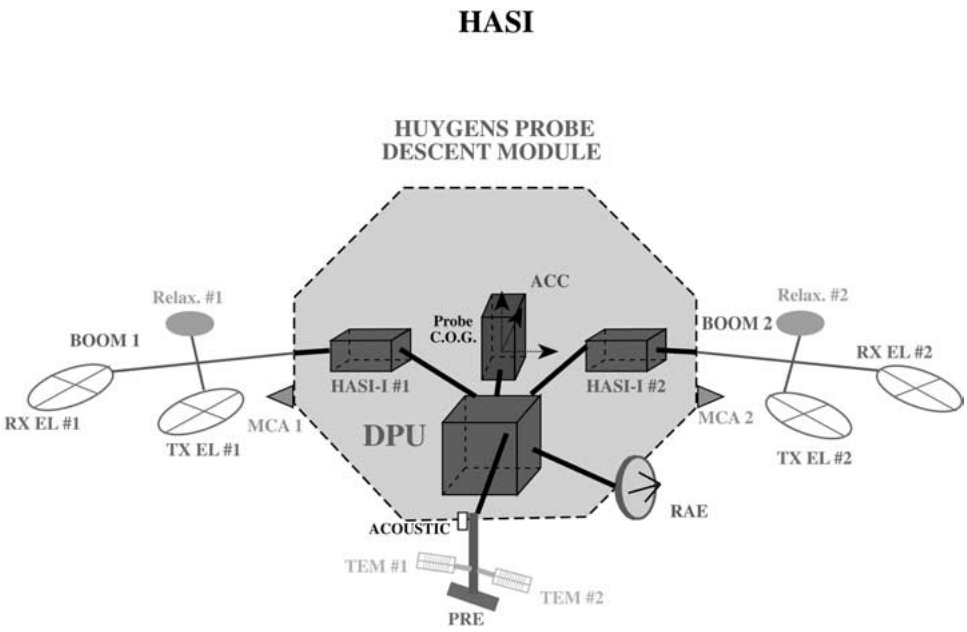

Figure 1. Block diagram of the HASI experiment on the Huygens probe in descent configuration (for acronyms refer to Tables I & II).

2.1.3. *STUB*

The STUB consists of a stem fixed on the Huygens ring (Figure 6), which is under the thermal shield of the Huygens probe during cruise phase. The STUB ensures that the sensors (two thermometers and a Kiel probe) are appropriately located and oriented with respect to the gas flow during the measurements. A microphone, the PWA acoustic sensor, is fixed on the STUB flange.

2.1.4. *Data Processing Unit (DPU)*

The DPU is the HASI electronics box located on the Huygens experiment platform close to the STUB. It is composed of four functional blocks:

- the PPI electronics board containing the pressure heads and the conditioning electronics;
- the Radar Altimeter Extension (RAE) board which is mounted on the PPI board and processes the return signal of the Huygens proximity sensor, before these data are spectrally analysed by the PWA electronics;
- the Permittivity, Wave and Altimetry (PWA) block (composed of two boards: analogue and digital) which provides the analogue signal conditioning and data conversion and processing for all PWA sensors;
- the Experiment Power Data Handling block (composed of four boards and one motherboard), which provides the power supply for the HASI subsystems, interaction between the electronics boards, TEM and ACC sensors conditioning

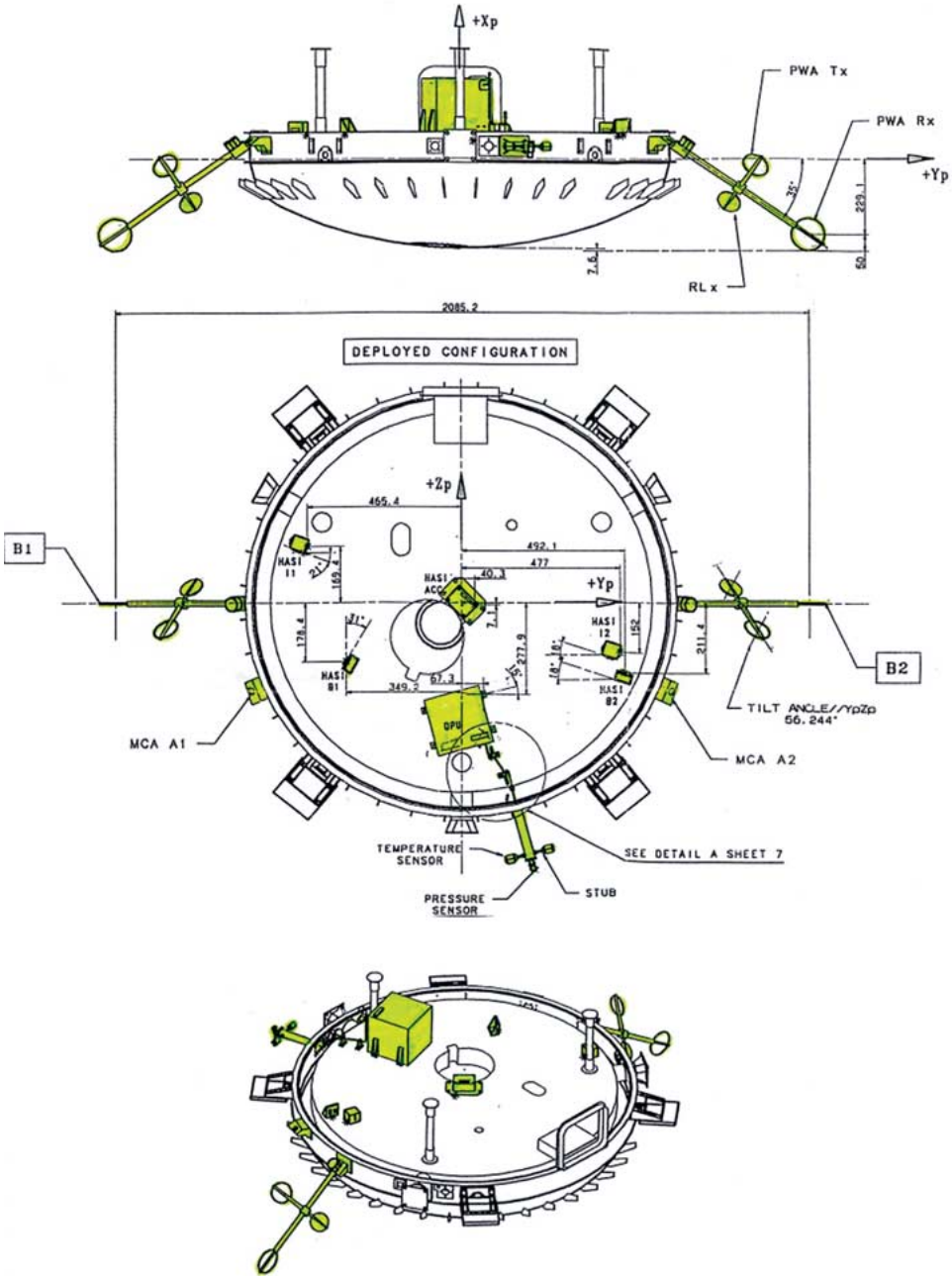

Figure 2. HASI subsystems accommodation on the experiment platform of the Huygens probe. TEM, PWA sensors and the Kiel probe of PPI are mounted outside the Huygens probe. The booms, carrying the PWA sensors, are stowed under the thermal shield of the probe during the interplanetary cruise and are deployed at the beginning of the descent into Titan's atmosphere. The STUB ensures that the temperature sensors and pressure inlet are appropriately located and oriented with respect to the gas flow during the measurements. The ACC box is located on the Huygens probe experiment platform, at the centre of mass of the Huygens probe in entry configuration.

TABLE II
HASI sensor packages

Sensor package	Acronym	Sensor type	Accuracy	Resolution	Measured parameters
Accelerometers*	ACC	3-axes accelerometer (1 X-servo & 3 piezo-resistive accelerometers)	1%	1–10 μg (high res.) 0.9–9 mg (low res.)	Atmospheric deceleration Descent monitoring Response to impact
Pressure Profile Instrument	PPI	Kiel type pressure probe + capacitive transducers	1%	0.01 hPa	Atmospheric pressure
Temperature sensors	TEM	2 dual element Pt thermometers	0.5 K	0.02 K	Atmospheric temperature
Permittivity, Wave and Altimetry	PWA	Mutual Impedance AC field measurement	10%	10^{-11} $(\Omega m)^{-1}$ 2μV/m (threshold)	Atmospheric electric conductivity Wave electric fields and lightning
		Relaxation probe	10%	1 min 25 ms - 2 s 1 mV (threshold)	Ion conductivity & DC electric field
		Acoustic sensor	5%	10 mPa (threshold)	Acoustic noise due to turbulence or storms
		Radar signal processing (FFT)	1.5 dB	40 m @24 km	Radar echoes below 60 km

*Figures for resolution and accuracy are for the X servo accelerometer.

and data conversion, data acquisition and processing, and experiment data handling to the Probe Command Data Management System.

2.2. HASI SENSOR PACKAGES

2.2.1. *ACC*

The Accelerometer subsystem consists of one highly sensitive single axis accelerometer (servo) and three piezoresistive accelerometers. The accelerometers are aligned parallel and perpendicular to the Huygens probe axis of symmetry. The servo is mounted at the Huygens probe's centre of mass, in order to sense change in acceleration along the probe's descent axis (X axis). The three piezoresistive accelerometers are mounted orthogonally, oriented along the probe's X, Y, and Z

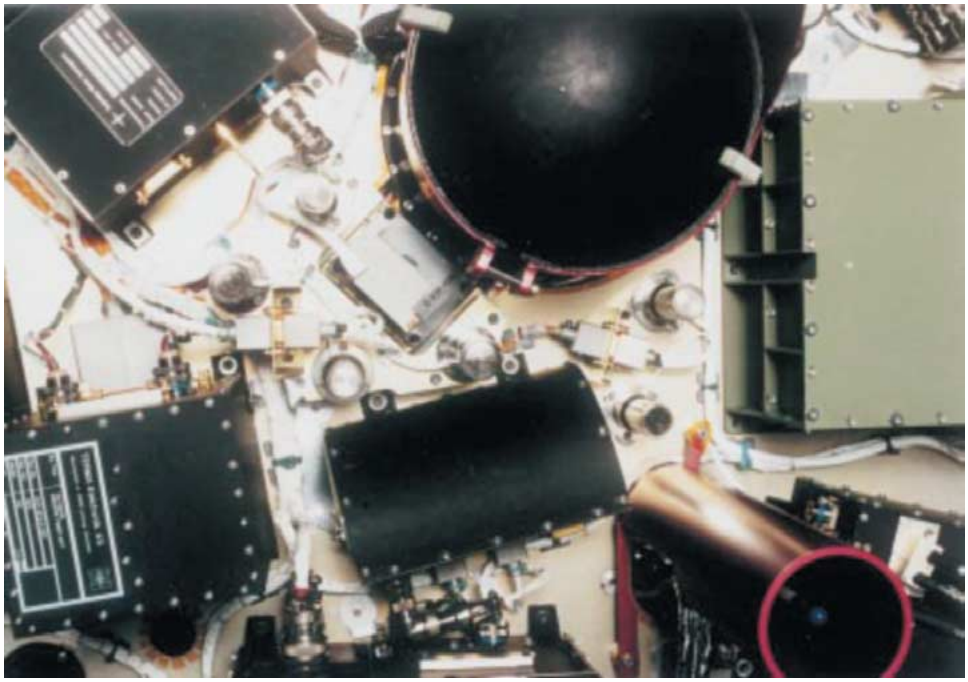

Figure 3. ACC subsystem mounted on the experiment platform of the Huygens probe.

axes. Temperature measurements are carried out by two AD 590 sensors in thermal contact with the accelerometers.

The servo accelerometer (Sundstrand QA-2000-030) senses the displacement of a seismic mass and drives it back to a null position; the required current is a direct measurement of acceleration. This package is gas filled and sealed to provide damping of the proof mass when deflected. The servo accelerometer output is amplified by two non-inverting amplifiers providing two channel outputs. In addition, the two channels have a switchable range (high and low resolution) by means of a single analogue switch. The absolute accuracy of the sensor is ± 35 μg in high resolution, high gain. The resolution is 1 to 10 μg, depending on the mode.

The piezo accelerometers (Endevco 7264A-2000T) consist of a suspended seismic mass supported by a cantilever whose displacement is determined by two strain-dependent resistances. The accelerometer is part of a Wheatstone bridge; the variation in voltage output produced when an external voltage is applied is dependent on acceleration. The strong dependence on temperature is compensated through the temperature measurement of the AD 590 sensor. The piezo accelerometers can resolve 0.1 g and provide an absolute accuracy of ± 0.4 g. The accuracy of the temperature diodes is ± 0.5 K.

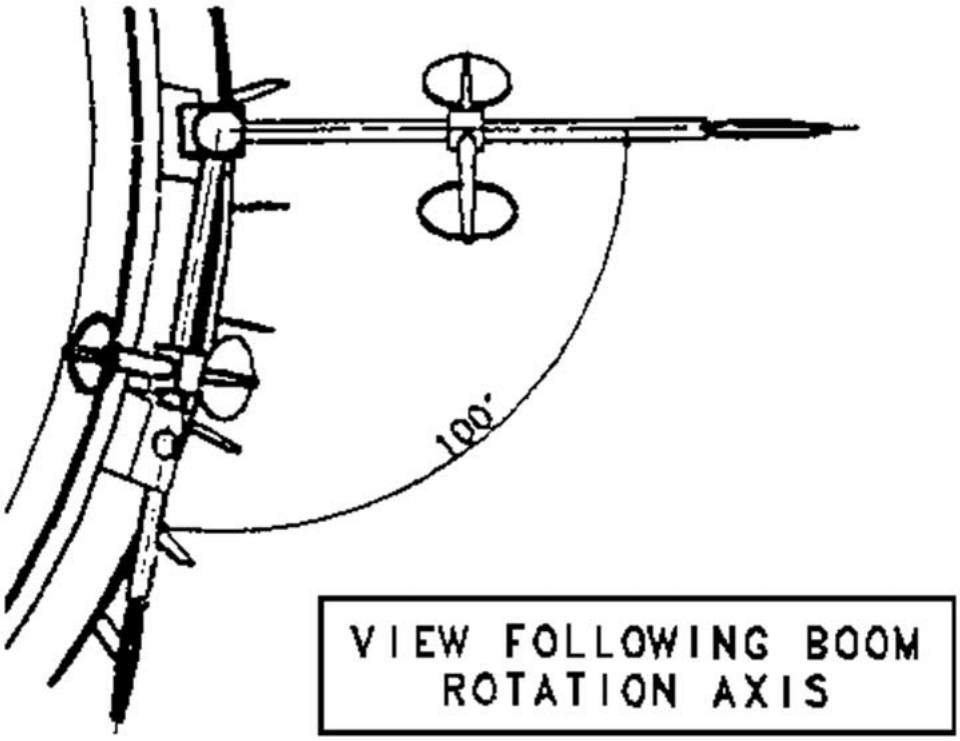

Figure 4. One unit of the Deployable Boom System carrying the PWA sensors in stowed and deployed configuration.

2.2.2. *TEM*

The HASI temperature sensors (TEM) are dual element platinum resistance thermometers (Ruffino *et al.* 1996; Angrilli *et al.*, 1996), manufactured by Rosemount Aerospace Inc., Minnesota, U.S. Each unit (Figure 7) is composed of a platinum-rhodium truss cage frame exposing the two sensing elements to the atmospheric flow. The principal sensor (fine) is a double platinum (Pt 99.999%) wire of 0.1 mm in diameter and 2 m in length, wound around a Pt-Rhodium frame from which it is insulated by a thin layer of glass. The secondary (coarse) sensor, designed as a spare unit in the case of damage on the primary sensor, is a thinner Pt wire (0.02 mm) annealed in the glass on the frontal side of the upper part of the frame. In order to include the TEM units in the global Huygens Faraday cage and to reduce electric noise, the sensors are coated with 25 μm of paralyne and 1 μm of gold. The two redundant TEM units are mounted on the STUB. The TEM sensors can resolve 0.02 K with an accuracy of 0.5 K at the best.

2.2.3. *Pressure Profile Instrument (PPI)*

The Pressure Profile Instrument includes sensors for measuring the atmospheric pressure during descent and surface phase (Harri *et al.*, 1998). The atmospheric

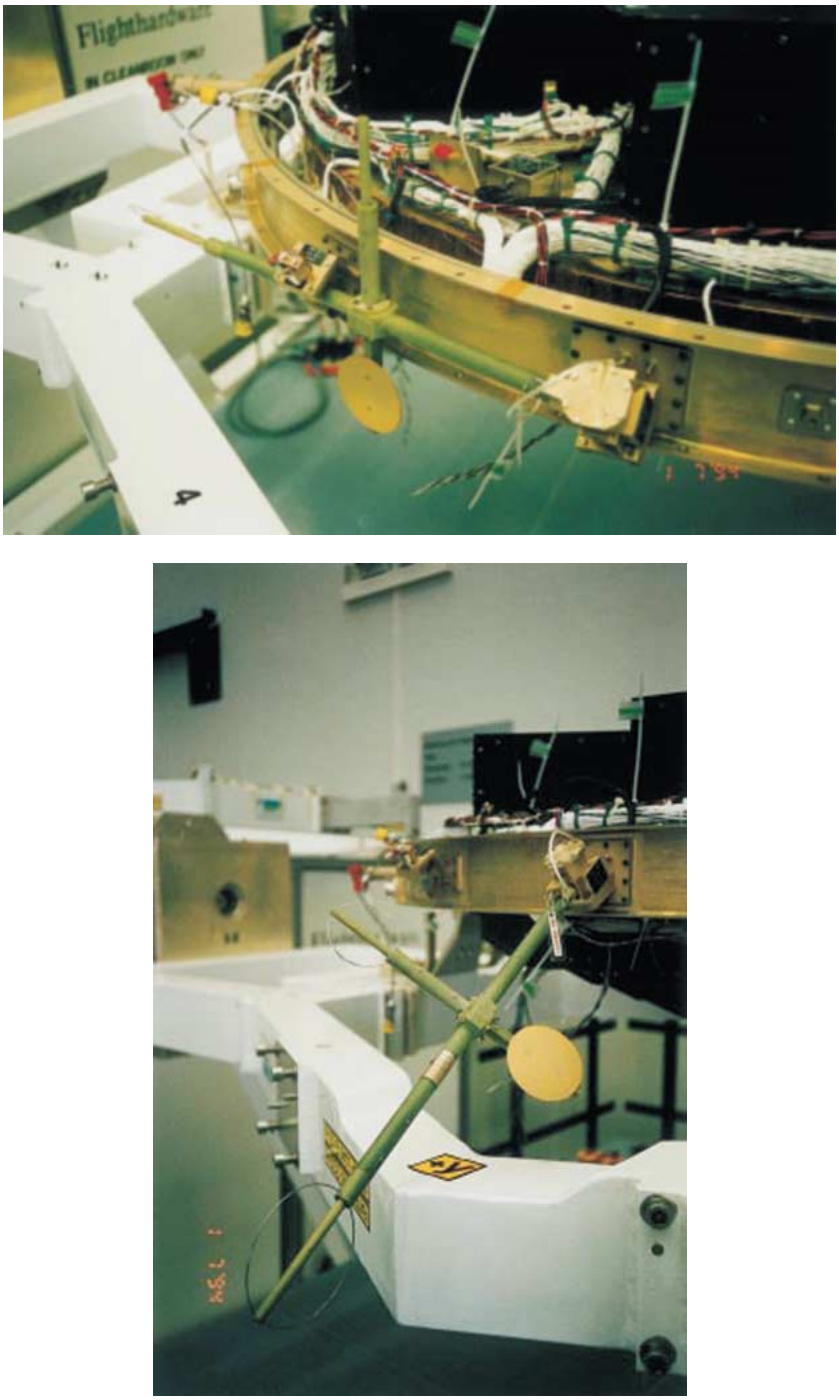

Figure 5. One component of the Deployable Boom System with the PWA sensors. In Figure A, the boom is locked (cruise configuration under the thermal shield). In Figure B, the boom is deployed (descend configuration). The three PWA electrodes are visible: the two rings are elements of the receiving antenna (RX, at the tip) and transmitting antenna (TX) for mutual impedance measurements; the disk forms the relaxation probe (RP). The RX and RP electrodes are connected to the preamplifiers contained in the HASI-I boxes (visible in Figure A on the probe experiment platform).

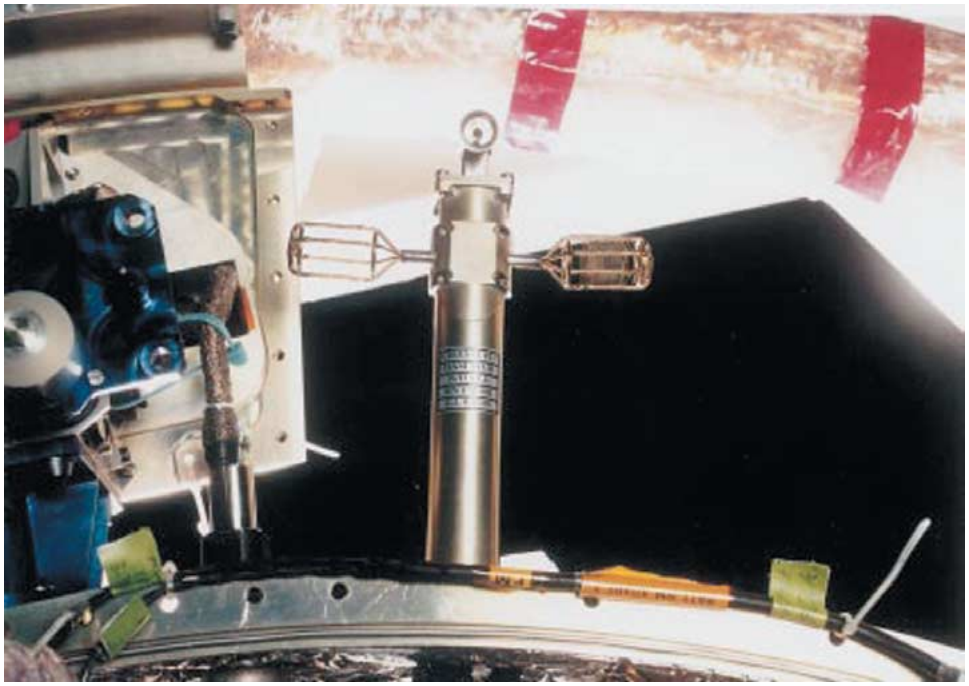

Figure 6. View of the flight model of the HASI STUB fixed to the Huygens probe ring during the testing and verification campaign.

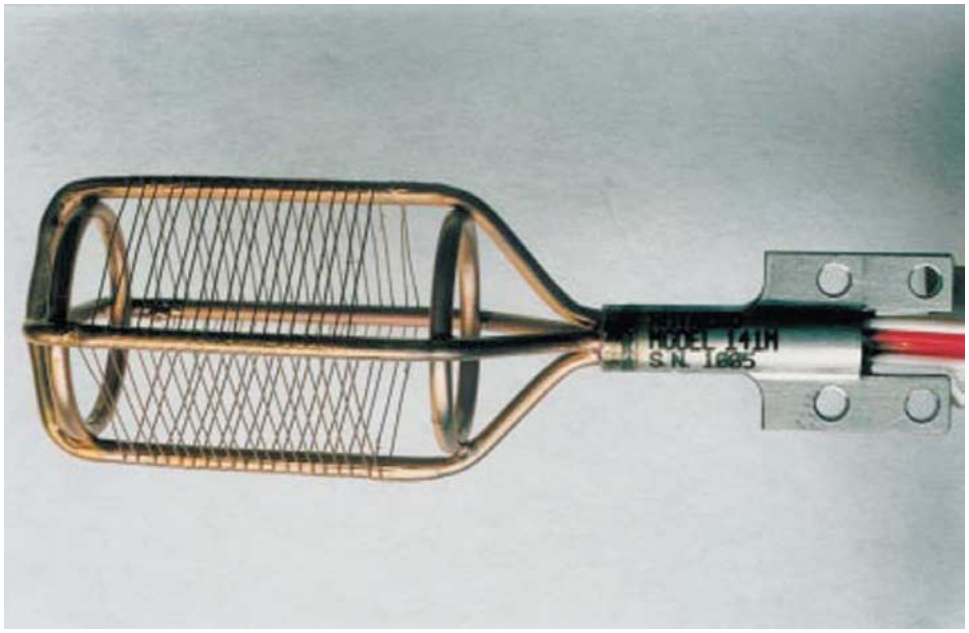

Figure 7. TEM sensor.

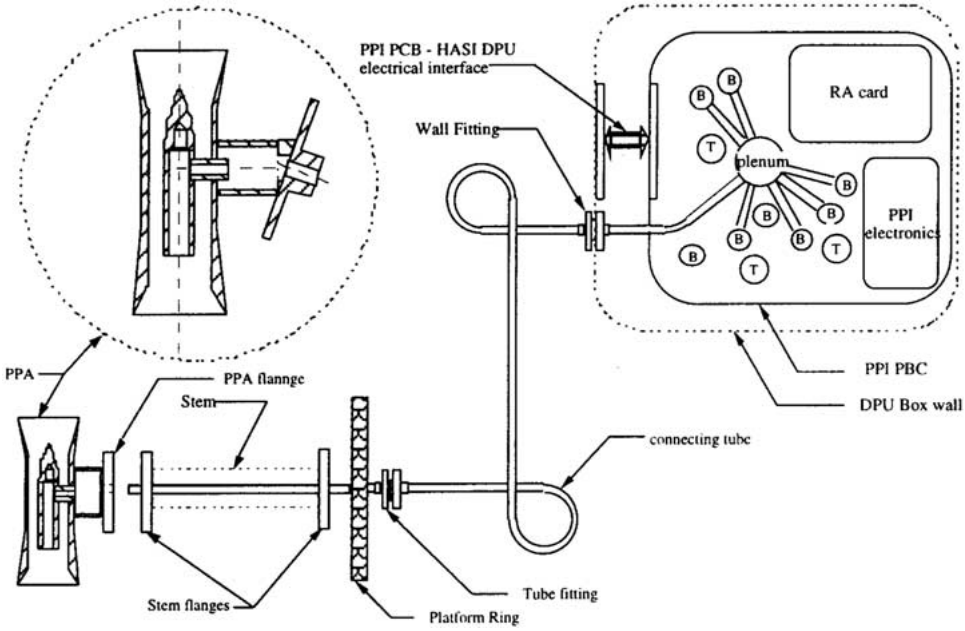

Figure 8. Schematic view of PPI assembly.

flow is conveyed through a Kiel-type pressure probe accommodated within a pitot tube, mounted on the STUB stem end, and is connected with a tube to the DPU, where the transducers and the related electronics are located (Figure 8). The Kiel probe has been designed to provide accurate measurements of total pressure (environmental plus kinetic pressure) even for variations in a flow inclination angle up to 45°. The pressure transducers are silicon capacitive absolute pressure sensors (Barocap) produced by the Vaisala Co, Helsinki, Finland. The Barocap consists of a small sensor head with associated transducer electronics. The varying ambient pressure deflects a thin silicon diaphragm in the sensor head, causing changes in the separation of two capacitive plates. The capacitance variation is converted into an oscillation frequency in the PPI electronics. Three types of Barocap, characterised by different thickness of silicon diaphragm, are used in order to cover the measurement range. The sensors with the thinnest diaphragms are used for high resolution, in the range 10^{-3}–10^{-2} hPa. The temperature dependence of the Barocap response is compensated by measuring the sensor temperature with Thermocap sensors. PPI sensors are connected to three oscillator blocks based on Vaisala Multicaps, each having eight frequency input channels. The first group contains sensors for intermediate pressure measurements with sensibility range from 0 to 1200 hPa, the second group for high pressure (0–1600 hPa) and the third for low pressure (0–400 hPa). In each Multicap, two channels are reserved for reference capacitors, R1 and R2, used for the reconstruction of pressure measurement; the other channels are

for sensors (Barocap and Thermocap). The accuracy of the pressure measurement is about 1% and the maximum resolution is 0.01 hPa.

2.2.4. *Permittivity, Wave and Altimetry package (PWA)*
The PWA sensors are six electrodes and an acoustic pressure transducer (Grard *et al.*, 1995). After the deployment of the booms, the two couples of the mutual impedance transmitter (TX) and the receiver (RX) electrodes form a trapezoid in the plane of the Huygens probe X-axis. The mutual impedance is measured by applying a sine wave pulse with amplitude 0.1–10 V at fixed frequencies (from 45 Hz up to 5.7 kHz after impact) on the two TX electrodes; amplitude and phase of impedance are computed using the analysis of the RX electrodes differential signal. A Fast Fourier Transform (FFT) is performed every 60 ms, with a 45 Hz spectral resolution in a 9.5 kHz bandwidth. The RX signal is also used in a passive mode to detect natural waves. The PWA quadrupolar probe will measure atmospheric electric conductivity due to the free electrons and detect wave emission in atmosphere and related phenomena such as lightning. Quasi-static electric field and ion conductivity will be measured through the relaxation probe. Positive and negative potentials will be applied between the descent module and the relaxation probe during a period of 1 s, every 1 min by closing switches; when the switches are open, the sensors and the vehicle discharge independently and return to their equilibrium potentials. From the measurement of these potentials as a function of time, positive and negative ion conductivities can be derived and the free electrons detected, if any. The relaxation electrodes are grounded at the end of the measurement sequence.

The acoustic sensor, mounted on STUB will detect sound waves to correlate with acoustic noise, turbulence, and meteorological events (pressure level threshold: 10 mPa).

The radar return signals of the Huygens Proximity Sensor, containing information on surface properties and altitude, are processed also by the Radar Altimeter Extension (RAE) board in the HASI experiment. The Huygens Proximity Sensor is composed of two Frequency Modulated Continuous Wave (FMCW) altimeter radars with redundant channels at 15.4 and 15.6 GHz respectively, operated to keep the intermediate frequency (IF) at 200 kHz. The transmitted signal is modulated in frequency with rising and falling ramp waveforms. Inside the RAE board, the radar return signal is converted to 10 kHz and filtered before passing to the PWA A/D converter and signal processor. The Huygens radar input signals in HASI/PWA (Figure 9) are the digital blanking signal and the analogue intermediate frequency signal (echo signal). The blanking signal is used to control the radar lock status and contains the altitude information, while information on surface properties can be retrieved from the analysis of the echo signal.

The PWA signal processor performs FFT, digital integration and data packetising and controls the data acquisition. The operational mode, and therefore the FFT analysis type, is selected depending on the altitude levels. An averaged spec-

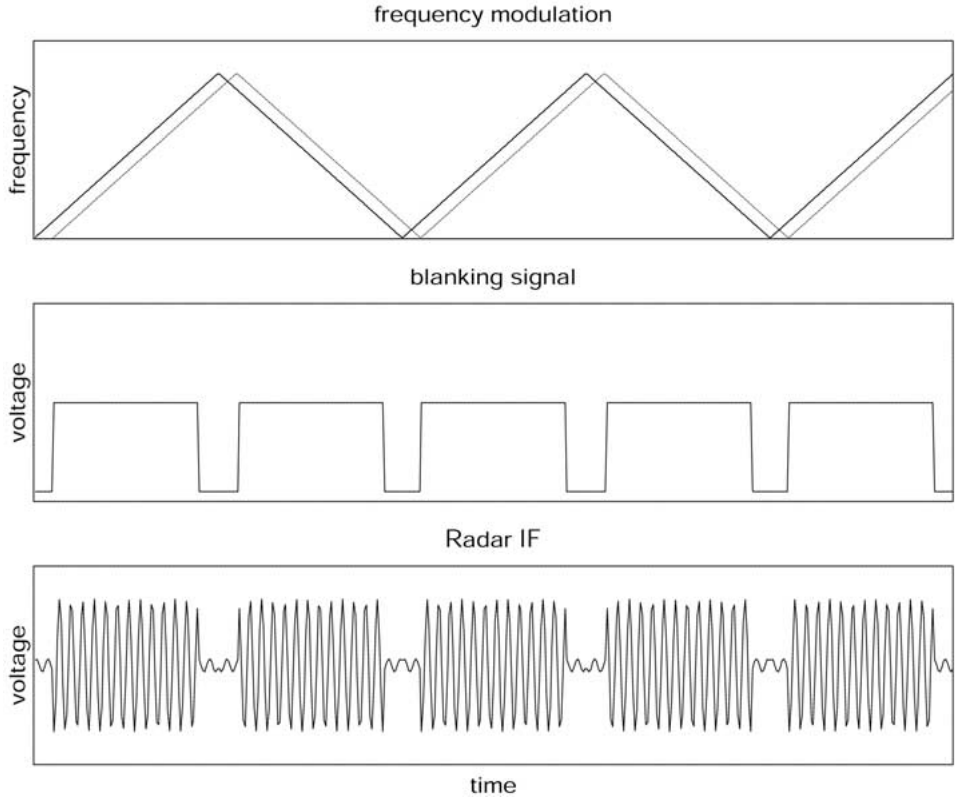

Figure 9. Radar signals of the Huygens proximity sensor transmitted to HASI for processing and elaboration.

trum is calculated separately for the rising and the falling ramp because of Doppler shift. Spectrum and altitude information of the return signal are added to the HASI data stream.

3. HASI Operations and Measurements

HASI will be the first instrument to perform measurements during the probe entry phase in Titan's atmosphere. HASI is switched on during the coast phase of the Huygens probe to Titan, ten minutes before the beginning of the entry phase. At two minutes after switch-on and during the entire high-speed entry phase, from an altitude 1300 km down to 160 km (∼4 min duration), acceleration data are sampled. After the probe has decelerated to Mach ∼1, the entry phase ends and the probe device deployment sequence begins. In a period of three minutes the pilot parachute is fired to lift off the probe aft cover and inflate the main parachute; the frontal thermal shield is released falling away. From this moment, starting from 160-km altitude, the Huygens scientific instruments are exposed to Titan's

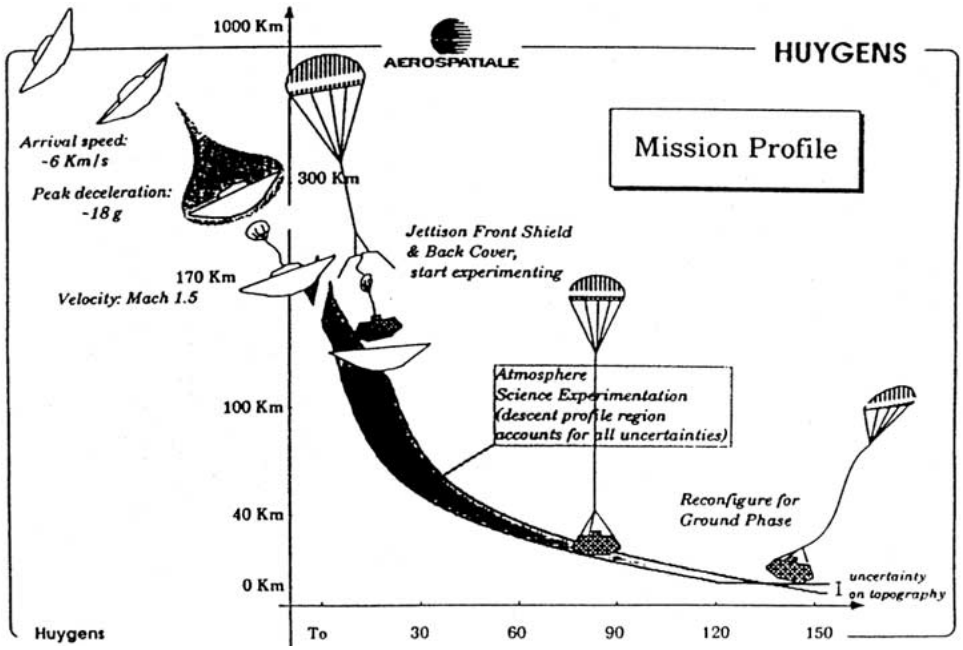

Figure 10. The Huygens mission profile at Titan: entry and descent sequence of the Huygens probe in Titan's atmosphere.

atmosphere. The probe descent continues on parachute. At 120-km altitude, the main parachute is cut away and replaced by a smaller one. The complete descent will last 2 h and 15 min. At least, another 15 min are foreseen to perform surface measurements after landing, before the batteries run out and/or the probe relay link to the orbiter is lost. The Huygens mission scenario is reported in Figure 10.

Given the atmospheric mean molecular weight and the probe aerodynamics, vertical profiles of density, pressure, and temperature can be derived from the three axes accelerometer data (Seiff *et al.* 1980, 1997b, 1998). About one minute after the frontal shield release, the HASI booms are deployed and direct measurements of pressure, temperature and electrical properties are performed.

The sampling of HASI sensors is driven by a predetermined time sequence that is triggered by environmental conditions during descent. Proximity sensor sampling will start at 60-km altitude, but the probe system will continue to use the altitude table until both the radars lock (anticipated to be at about 30 km). In that part of the atmosphere, PPI will switch from low to medium sensitivity channels and then to its high-pressure channel. The PPI measurement cycle is organised in a sequence of normal and burst sessions; in normal mode, 9 samples are recorded in 43.2 s and average and standard deviation of five values are computed, in burst mode 19 samples for sensor are recorded in six seconds. The effective temporal resolution is between 2.4 and 4.8 s.

In the last km (HASI impact mode) the ACC will be reset to impact detection, acceleration data will be stored for transmission after the impact. In this last part of the atmosphere, only the TEM fine sensors will be sampled every 1.25 s in order to achieve a better vertical resolution. The normal sampling (4 measurements alternating fine and coarse sensors sample of TEM1 and 2 on a period of 5 s) will be selected again at the surface.

4. HASI Contribution to the Huygens Trajectory Reconstruction

Reconstruction of the probe entry and descent trajectory is needed in order to correctly interpret and correlate the results from all Huygens science experiments and to calibrate the remote sensing measurements from the orbiter instruments. HASI will measure the atmospheric pressure and temperature as well as the profile of axial and normal accelerations during the Huygens descent in Titan's atmosphere, so that it will mainly contribute to the descent trajectory reconstruction analysis. Its acceleration data and then direct pressure and temperature measurements will provide fundamental information for reconstructing the height versus time profile.

Using the assumptions of hydrostatic equilibrium and the equation of state, pressure and temperature will be used to determine the probe descent velocity. During the entry phase, the determination of the atmospheric vertical profiles requires the reconstruction of the probe trajectory and of the velocity temporal history. The probe trajectory and attitude can be reconstructed by analysing vehicle acceleration by an accelerometer aligned parallel and perpendicular to the probe symmetry axis. During the high-speed entry phase, the probe entry track, velocity and altitude profiles, and attitude will be retrieved from acceleration data in redundancy with the measurements of the Huygens housekeeping accelerometers (these sensors are less accurate than the HASI ones).

During the descent, temporal velocity and altitude profiles will be derived from the pressure and temperature measurements performed by the HASI PPI and TEM, while the data of the three-axial accelerometer ACC will contribute to determine the probe drift and its motion induced by rotation and turbulence. In addition, the HASI elaboration of the radar return signal will provide an independent estimation of probe altitude and descent velocity in the troposphere approximately beneath 30 km. In the first part of the Huygens mission, during the probe entry in atmosphere (from about 1300 km to 160 km), the equations of motion will be integrated using the accelerometer data to derive probe velocity, flight path and azimuth angle as a function of time, starting from the probe initial conditions derived from navigation data and possibly imaging by the Cassini camera.

The parachute deployment and separation sequence and the opening of the thermal shell of the probe will imply an uncertainty on the trajectory determination. The accelerometer measurements could be saturated because of the pyro shocks, the cover releases, the chute deployment and separation and the jettison of the

thermal frontal shield beneath the probe could strongly affect the free fall of the probe, which in a few seconds (about 60 s) is changing its configuration. Then the probe will continue its descent dragged by the main parachute. From this point on, probe descent velocity can be derived primarily from HASI measurements of pressure and temperature, the assumption of hydrostatic equilibrium and the equation of state, and the known mean molecular mass (e.g., derived from the speed of sound measured by SSP):

$$V = \frac{dz}{dt} = \frac{RT}{\mu g} \frac{\partial \ln P}{\partial t} \tag{1}$$

Height versus time profile can be derived integrating the descent velocity or the hydrodynamic law:

$$z = \int_{P_0}^{P} \frac{RT}{\mu g} \frac{dP}{P} \tag{2}$$

where $P_0$is the pressure at the surface level. These techniques have been applied in the atmosphere of Mars, Venus and Jupiter (Seiff *et al.*, 1980, 1997b, 1998).

In the lower atmosphere the Huygens radar altimeter, starting approximately at 33 km (the altitude at which the lock of the radar signal is foreseen), will derive the altitude from surface level and the descent velocity. The integration process of the equations of motion for the trajectory reconstruction is continuous, iterative and inverse, from the surface up to the beginning of the descent. The satellite surface is the lower boundary condition of zero velocity and 'known' altitude used to correctly scale the estimated values.

5. HASI Expected Results

The scientific measurements performed by HASI are designed to characterise Titan's environment. The main scientific objectives are:

- Determine the atmospheric pressure and temperature profiles.
- Evaluate the density profile and molecular weight profiles.
- Determine the atmospheric electric conductivity and charge carrier profiles.
- Investigate ionisation processes.
- Survey the wave electric fields, atmospheric lightning and analyse the quasi-static electric fields leading to storm formation.
- Detect acoustic noise due to turbulence or thunder.
- Characterise the roughness, mechanical and electric properties of the surface material, whatever its phase, solid or liquid.

The three-axis accelerometer ACC, placed at the centre of mass of the Huygens probe, will record the atmospheric deceleration and the impact trace with a resolution as high as 1 μg. The total pressure and temperature will be monitored by

the PPI and TEM sensors, which sample the undisturbed field outside the probe boundary layer. The Kiel probe and the PPI capacitive gauges will sample the pressure with a resolution of 0.01 hPa, while the platinum wire thermometers, TEM, will measure temperature with an accuracy of 0.5 K and a resolution of 0.02 K.

HASI deceleration data will provide information about the energetic balance of the thermosphere and will contribute to the investigation of the physical conditions of the high stratosphere where methane dissociation takes place and the haze is formed (Hunten *et al.*, 1984). About 1 min after the Huygens frontal thermal shield separation, at a height level of about 160 km, the HASI booms will be deployed and direct measurements of pressure, temperature and electrical properties will be carried out through Titan's stratosphere and troposphere, down to the surface, for the entire duration of the descent (nominally 2 h and 15 min) and for at least 15 min after landing.

HASI data will contribute also to other investigations of Titan's environment, such as atmospheric composition analysis and the study of the vertical distribution of organic and inorganic compounds. Moreover they will provide a reference for the calibration of some remote sensing observations from the orbiter (i.e. radio occultation, IR spectroscopy) and measurements of other experiments on-board the Huygens probe.

5.1. ATMOSPHERIC STRUCTURE

Determination of temperature and pressure profiles, also combining HASI measurements with data of other experiments, will help to define the atmospheric structure (Lellouch *et al.*, 1990; Yelle, 1991), layer by layer composition (in particular to evaluate the CH_4 mixing ratio in the saturation region), the vertical concentration profile of organic and inorganic compounds (Coustenis *et al.*, 1989, 1991, 1995a; Lara *et al.*, 1996), and the partial pressure of saturated gas in order to detect the presence of tropospheric clouds (Toon *et al.*, 1988) or supersaturation layers (Courtin *et al.*, 1995).

During the entry phase in Titan's atmosphere, the information on density, pressure and temperature will be derived indirectly from ACC deceleration measurements. In this phase the typical scale height ($H = \frac{RT}{\mu g}$) of Titan's atmosphere is thought to be about 40 km; the descent velocity is expected to vary from 6200 m s^{-1} to 400 m s^{-1} (Table III). In order to obtain a good resolution, three or four measurements per scale height are necessary (Fulchignoni *et al.*, 1997). The atmospheric density is directly related to the aerodynamic deceleration of the probe ($-a_p$):

$$\rho(z) = -\frac{2ma_p}{C_D A V_r^2} \tag{3}$$

where m is the mass of the entry vehicle, the aerodynamic drag coefficient C_D and the probe cross section area (A) are constants known from ground tests. V_r is the

TABLE III

HASI Timeline, probe events and related dynamic conditions during the Huygens mission

	Time (min)	Mission time	Altitude (km)	Vertical velocity ($m\ s^{-1}$)	Acceleration ($m\ s^{-2}$)		
COAST		T0 − 22d 5 mn				Tsep	*Probe separation from Orbiter*
		T0 − 18 mn				Tp	*Probe power-up and CDMS activities*
		T0 − 10 mn				Thasi	HASI ON (17:46 preT0)
		T0 − 8 mn				Tacc	ACC sampling start
ENTRY	0.03	∼T0 − 5 mn	1260.8	6145.28	0.61	Tentry	
	2.7		401.082	6114.32	11.031		
	3.37		229.334	3404.9	120.78	max acc	
	4.13		170.24	638.54	16.886		
	4.42		162.648	429.37	8.3181		
DESCENT							*End of entry phase*
	0.03		162.063	307.91	24.196	T0	*Descent device deployment begins*
		T0 + 00.25 s					*Pilot chute deployed and inflation*
		T0 + 2.5 s					*Back cover release, main chute deployment & inflation*
	0.5	T0 + 32.5 s	157.452	99.63	2.469		*Front shield jettison*
	1	T0 + 1 mn					*DISR cover jettison*
	1.05		154.904	67.42	0.598	Tdata, Td1	T&p sampling; 1st BOOM release attempt start
	1.55		153.002	62.06	0.255	Td1w	1st BOOM release attempt end
	2.2		150.658	59.72	0.113	Td2	2nd BOOM release attempt start
	2.5		149.775	59.08	0.086	TdataH	PWA sampling (mode A) start
		T0 + 15 mn	114.733	36.61	0.02		*Main chute jettison, stabiliser deployment & inflation*
	25.78		74.906	44.58	0.049		
	32.12		61.372	27.49	0.028	Tradar	RADAR sampling, PWA mode C
	48.45		42.103	14.71	0.007	tropo-pause	
	75.12		24.262	8.76	0.002	Tpmed	Medium p sampling start
	105.1		11.034	6.29	0.001	Tphigh	High p sampling start
			7				PWA mode D (no RP)
	134.5		1.025	5.22	0	last km	IMPACT mode
	138.1		0	0	0	IMPACT	SURFACE mode, PWA mode G
						Tloss	*Loss of radio link*

probe velocity relative to atmosphere. Combining (3) with the hydrostatic equation, and knowing the molecular mean mass, temperature can be calculated. The pressure and temperature profiles measured during the descent can be incorporated into the hydrostatic law, to calculate the absolute heights from the surface of Titan as a function of time. These techniques have been applied for the investigation of other planetary atmospheres, e.g., Venus by Pioneer probes (Seiff *et al.*, 1980), Mars by Pathfinder (Seiff *et al.*, 1997b; Schofield *et al.*, 1997), Jupiter by Galileo probe (Seiff *et al.*, 1998).

Pressure and temperature measurements obtained during the parachute descent phase must be corrected taking the dynamic conditions into account. The dynamic correction of the measured profiles can be carried out with an iterative process described in Fulchignoni *et al.*, (1997).

During the entry phase HASI will perform on average one acceleration measurement every 128 m; from these data, information on the upper stratosphere will be derived in order to investigate the physical conditions present in the region

where CH_4 is photodissociated and the haze is formed (Hunten *et al.*, 1984). In order to define the layer-by-layer composition of this part of the atmosphere, where more complex organic compounds are built up and some species could condense (Sagan and Thompson, 1984; Coustenis *et al.*, 1995a), accurate local measurements of the stratospheric pressure and temperature profile are needed. To reach this goal, at least one measurement every 4 km was requested (Fulchignoni *et al.*, 1997); HASI will take a measurement every half kilometre. Combining the HASI data with those of other experiments, it will be possible to derive the atmospheric chemical composition as a function of altitude, to provide the vertical concentration profile of inorganic and organic compounds and also to contribute to the analysis of the chemical composition of the aerosol gathered and analysed by the ACP (Israel *et al.*, this issue) and GCMS (Niemann *et al.*, this issue). Moreover HASI data will contribute to estimates of the mixing ratios to identify the condensates. In order to determine if the partial pressure of a specific compound is equal to its saturation vapour pressure and consequently if it could condense at a certain height, an accurate knowledge of the temperature conditions is needed. HASI could detect the presence of methane clouds at the level of the 'cold trap', where the minimum atmospheric temperature value is reached (the tropopause: 40 km, 71 K) (Lellouch *et al.*, 1990; Yelle, 1991). At these heights the Huygens probe, dragged by the pilot chute, will continue to descend at a speed of about 15 m s^{-1}, so that HASI measurements will have a good spatial resolution on the typical scale height of about 16 km (at least one measurement every 35–40 m).

In the lower atmosphere HASI will accurately sample the pressure and temperature profiles (about one measurement every 5 m) in order to determine the vertical temperature lapse rate. Based on Voyager observations, the lapse rate is expected to be very close to the radiative equilibrium value; less than the dry lapse rate ($\frac{dT}{dz} = 1.3$ K/km) but larger than the moist lapse rate (McKay *et al.*, 1997). Convective zone is expected to extend only a few kilometres above the surface (McKay *et al.*, 1989). Direct detection of the temperature lapse rate will provide confirmation of the convective and condensation properties of the troposphere on Titan. Combining the HASI temperature data with the solar flux measurements performed by DISR (Tomasko *et al.*, this issue), it will be possible to evaluate the thermal balance of Titan's atmosphere.

HASI temperature and pressure sounding capabilities are reported in Figure 11 together with the temperature profile of Titan's atmosphere as derived from the tropospheric structure model of Lellouch *et al.* (1990). HASI vertical resolution depends on the probe descent velocity and sensor sampling rate. In the upper atmosphere, where temperature and pressure are derived from acceleration data, HASI resolution is of the order of 2 km, then it will gradually decrease to a few meters in the troposphere. The two 'inversions' at 160 km and 115 km correspond to the deployment of pilot and drogue chutes.

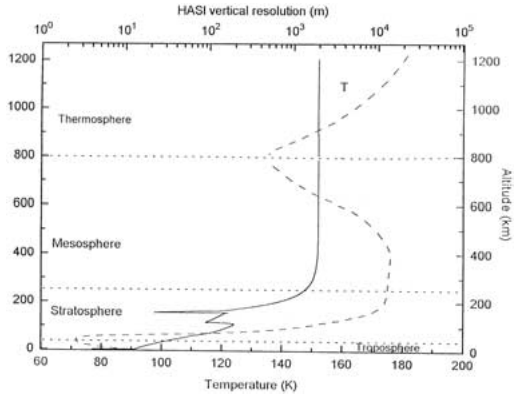

Figure 11. HASI temperature and pressure sounding capabilities. The spatial resolution of temperature and pressure measurements derived from HASI data during the entry and descent in Titan's atmosphere is reported as a function of the altitude from the surface level. The dashed line represents the vertical temperature profile (Lellouch *et al.*, 1990).

5.2. ATMOSPHERIC DYNAMICS

Acceleration, pressure and temperature measurements provide information about wind, gravity waves and turbulence in the atmosphere or at least allow deducing if conditions leading to turbulence were present. Assuming that turbulence is important only when turbulent diffusion is stronger than molecular diffusion, the minimum turbulence intensity in Titan's atmosphere can be estimated. In order to detect scale lengths associated to turbulence (min and max dimensions of the turbulence cell), the HASI accelerometer should measure scale lengths decreasing from a value of 50 km at 1000 km altitude down to 0.5 km at the troposphere (Fulchignoni, 1992). The actual HASI accelerometer capabilities ensure spatial resolution of 2 km at an altitude of 1000 km, and vary from 8 m at the tropopause down to 3 m in the last kilometres.

Variations in the density and pressure profiles, as well as in the temperature lapse rate, give information regarding atmospheric layering, atmospheric stability, wind, wave propagation and saturation. Latitude variations in the temperature lapse rate observed by Voyager confirmed the existence of strong zonal winds close to the 1 hPa level that could have speeds between 50 and 100 m s^{-1} (Flasar *et al.*, 1981). Analysis of the observations of the 28 Sagittarii stellar occultation by Titan in July 1989 has demonstrated the presence of zonal wind with equatorial speed of 100 m s^{-1}, and also of structures reminiscent of gravity wave propagation (Hubbard *et al.*, 1993; Strobel and Sicardy, 1997). The oscillations in the derived density and temperature profiles are characterised by small amplitude with quasi-periodic vertical structures similar to gravity waves (Sicardy *et al.*, 1999). Currently, the poor knowledge of Titan's topographic elevation profile, wind system, and meteorology strongly constrains data interpretation in terms of gravity waves and the determination of the mechanisms that could produce gravity waves in Titan's at-

mosphere. HASI will provide in situ atmospheric density, pressure and temperature vertical profiles as well as the topographic elevation profile and surface roughness through the analysis of the radar altimeter return signal. These measurements will lead to a better understanding of Titan's environment and constrain the interpretation of the processes that occur in it, specifically in terms of waves and thermal tides.

Wind gusts in the atmosphere can be observed by monitoring the periodic oscillations of the probe-parachute system with the accelerometers and thus detecting any perturbations on these oscillations caused by wind (Seiff *et al.*1993, 1997a). These results could be compared and confirmed by the measurements of the Doppler Wind Experiment (DWE) (Bird *et al.*, this issue). The presence of thunderstorms or other meteorological phenomena, such as hail and rain (Lorenz, 1993), could be detected through the measurements made by the PWA acoustic sensor.

5.3. ATMOSPHERIC ELECTRIC PROPERTIES

Titan's atmosphere undergoes a constant bombardment of galactic cosmic rays and Saturnian magnetospheric particles giving rise to free electrons and primary ions. These charged particles are subsequently captured by aerosol droplets and form heavy ions, which accumulate in tropospheric clouds. Friction, fragmentation, or collisions during convective activity may increase the charged particle number. Charge separation due to convection and gravitational sedimentation induces electric fields within clouds and between cloud layers and the surface.

Nitrogen and methane are the main atmospheric compounds in Titan's atmosphere and the solar radiation flux input on Titan is only 1% of that on Earth (Borucki *et al.*, 1984). Our knowledge of the electric properties of Titan's atmosphere and an investigation of electrical phenomena associated with storm activity, such as electrical discharges, atmospheric currents, electric potential gradients, atmospheric conductivity and electrical charging of surfaces are necessarily exploratory.

The ionospheric electron density profile model, given in Figure 12, has been derived combining: (i) an upper layer due to the solar photon bombardment and the impact of magnetospheric electrons (Ip, 1990); (ii) a lower layer related to galactic cosmic ray ionisation (Borucki *et al.*, 1987); (iii) a hypothetical intermediate layer (height ~ 500 km) due to meteoritic impacts (Grard, 1997). Lindal *et al.* (1983), on the basis of Voyager 1 radio occultation measurement, gave an upper limit of 3.5×10^3 cm^{-3} for Titan's electron density.

The conductivity of Titan's atmosphere is probably higher than Earth's, owing to the fact that nitrogen and other atmospheric molecules do not form negative ions on Titan. In Figure 13 the atmospheric conductivity profiles are estimated from the plasma density model of Borucki *et al.* (1987) and the pressure and neutral profiles of Lellouch *et al.* (1990).

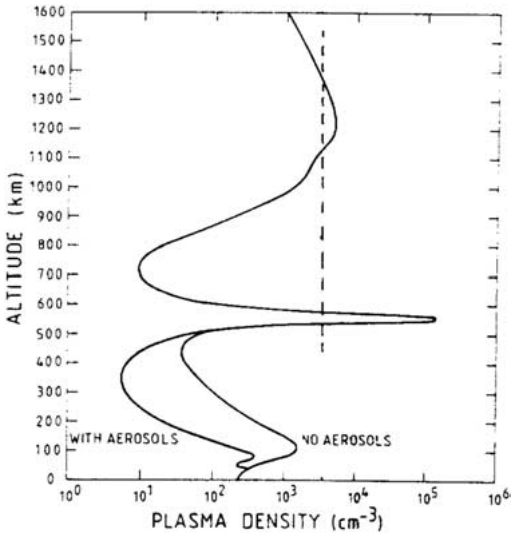

Figure 12. Vertical profile of the electron density in Titan's atmosphere. The dashed line is the upper limit derived from Voyager 1 radio occultation data (Grard, 1997).

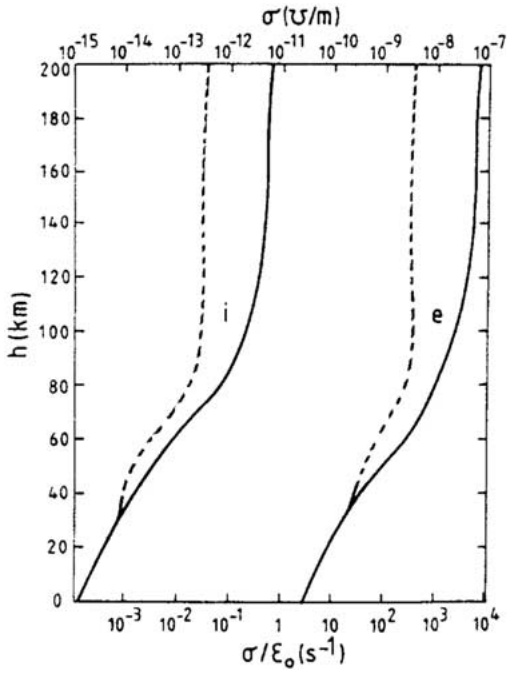

Figure 13. Models of ions (i) and electrons (e) conductivity profiles with and without aerosols (dashed and full line, respectively) (Grard, 1997).

Whistlers have been observed in the magnetosphere of other planets (e.g., Jupiter) and bear evidence of lightning activity (Rinnert, 1985). The absence of any substantial magnetic field on Titan does not allow waves to propagate in this mode; moreover, the electric fields may not be strong enough to produce lightning (Borucki *et al.*, 1984) and the convection energy could be dissipated through corona effects. Some form of electrical discharges may however take place in the height range 0–35 km (Boruki *et al.*, 1984; Navarro-Gonzales & Ramirez, 1998) and be the source of complex organic chemistry reactions.

The fact that no radio emissions were received during the Voyager 1 flyby, implies that lightning discharges on Titan are either infrequent or characterised by a different energy spectrum. An energy flash of the order of 10^6 J, 200–1000 times fainter than that of a typical terrestrial lightning event, should have been detected by Voyager (Desch & Kaiser, 1990). Radio wave emissions could have been shielded by a meteoritic ionised layer (Grard, 1997), which still has to be detected. Evidence for lightning activity and corona effects will be investigated with HASI, but detection of the associated electromagnetic emissions will be a function of the probe descent profile, the average discharge rate, and the typical discharge energy (Grard *et al.*, 1995).

The global effect of the electric phenomena could also excite the spherical resonant cavity limited by the satellite surface and the ionosphere lower boundary. The frequencies of the Schumann resonance are inversely proportional to the planetary body radius and 2.5 times greater on Titan than on Earth (Polk, 1982).

The scientific objectives of the measurements performed by the HASI PWA sensors package are: (i) studying the ionisation processes due to cosmic galactic rays, Saturn magnetospheric electrons and micrometeorites; (ii) investigating the electric charge production and transport mechanisms and determining the charge carrier density profiles; (iii) measuring electric fields and the ion and free electron conductivities, (iv) detecting and surveying wave electric fields and possible atmospheric lightning; (v) detecting acoustic noise due to turbulence and thunder (Grard, *et al.*, 1995).

Some phenomena will be directly measurable, others will be inferred from the observations; for example, the presence of atmospheric currents can be deduced from the atmospheric conductivity and electric potential gradient. Electromagnetic waves with frequencies lower than 100 kHz are confined within the ionospheric cavity and can be detected only *in situ* (Grard, 1997). The Schumann resonance spectrum yields information about the intensity and global properties of lightning activity and electromagnetic fields. During the descent and after landing, the mutual impedance measurements performed with the PWA quadrupolar probe will give the electrical conductivity of the free electrons in the atmosphere, and the two relaxation probes will measure the ion conductivity and provide information about quasi-static electric fields. Electron and ion densities will be derived from the conductivities, with the knowledge of the atmospheric neutral density and temperature.

5.4. SURFACE AND ATMOSPHERIC BOUNDARY LAYER CHARACTERISATION

The surface of Titan is hidden under a thick photochemical haze, which prevents direct observations. Titan's total density indicates rock and water ice as its principal components. The images of Ganymede and Callisto, satellites that have almost the same size of Titan, suggest that Titan's surface should be characterised by craters and topographic variations of the order of 1 km (Lunine & Lorenz, 1996).

The presence of hydrogen in Titan's atmosphere implies its continuous supply through the methane photolysis and, consequently, the existence of a methane reservoir. Lunine *et al.* (1983) proposed the existence of a global hydrocarbon ocean. Radar observations (Muhleman *et al.*, 1995), near IR observations (Griffith *et al.*, 1991; Coustenis *et al.*, 1995b) and the HST images (Smith *et al.*, 1996, Lemmon *et al.*, 1995) which penetrated the haze, show that Titan's surface is heterogeneous. These data argue against a global ocean, but are consistent with the presence of shallow lakes, formed by an accumulation of liquids in the bottom of crater basins (Lara *et al.*, 1994). Albedo variations observed in the near IR from ground and from HST seem to indicate the presence of two types of terrain: one darker and the other brighter than water ice. The Huygens probe will land on the western edge of one of these bright spots, about the size of Australia and centred near the equator.

If the probe survives the impact without losing the radio link, the HASI data will contribute to the characterisation of Titan's atmospheric boundary layer and surface, partly redundant with the experiment Surface Science Package (SSP) (Zarnecki *et al.*, this issue).

ACC will detect the probe impact on Titan's surface and will record the instant and impact trace, yielding indications on surface hardness. In the case of a 'liquid' landing, the accelerometer data will contribute to characterise the waves. The PWA quadrupolar probe will investigate the conductivity at ground level and, in case of liquid surface, the electric properties, conductivity and permittivity of the liquid. Pressure and temperature sensors will measure the surface conditions, contributing to the definition of the mean atmospheric molecular weight and the estimation of the amount of non condensable gas (e.g., nitrogen). In the presence of a liquid phase, the vapour pressure and the methane mixing ratios will be determined in order to evaluate the composition of the eventual sea or lake.

Spectral analysis of the radar altimeter return signals will provide the topography along the ground track of the Huygens probe descent, the medium- and small-scale surface texture and the spatial integrated value of the surface material permittivity. In general HASI data will help to discriminate between a liquid and a solid surface.

6. HASI Testing Campaign

The HASI experiment was tested following the assembly, integration and verification plan both at experiment and system levels, with the instrument integrated on the Huygens probe. Its performance was fully demonstrated through the qualification and acceptance test campaign, which included tests to simulate the extreme environmental conditions that the system will experience during the cruise phase and during the mission at Titan.

HASI sensors were characterised and calibrated at the subsystem level. In addition their performance has been verified through two balloon flights in Earth's atmosphere. Titan's atmosphere is thought to be very similar to Earth's in terms of pressure, density, and thermal structure, although the temperature values on Titan are much lower. A stratospheric balloon flight represents an excellent opportunity to test and verify the HASI performance, providing a realistic functional test in aerodynamic conditions similar to those of the Huygens probe descent on Titan.

6.1. THE COMA SOLA[1] BALLOON FLIGHT EXPERIMENT

The Instituto de Astrofisica de Andalucia in collaboration with the Instituto Nacional de Técnica Aerospacial (Spain) and the Centre National des Etudes Spatiales (France) organised the balloon flight of the COMAS SOLA experiment. The payload was a 1:1 mock-up of the Huygens probe on which all the HASI subsystems (refurbished breadboard or qualification models) and one Huygens radar altimeter unit have been integrated. The deployable booms carrying PWA electrodes, the radar altimeter receiving and transmitting antennas and the STUB were placed on the probe mock-up ring in the exact configuration of the Huygens flight model. The X-servo accelerometer, the electronic packages for data handling and storage of PWA, radar (RAE), pressure and temperature subsystems were located inside the mock-up, together with the battery and telemetry packages.

On December 1, 1995, a 35 000 m^3 balloon launched from the Léon base (Spain), brought the COMAS SOLA experiment to an altitude of 30 km (Figure 14). A daylight flight was scheduled in order to reach the maximum possible height and to recover the payload immediately after the flight. The flight baseline foresaw a quick rise (speed ~ 5 m s^{-1}) up to the ceiling, a drift period (maximum 15 min) at the highest altitude and a parachute descent divided in two phases: at low (3 m s^{-1}) and at high (11 m s^{-1}) speed, respectively. The balloon position along its trajectory was tracked by GPS (Global Positioning System) and OMEGA (triangulation with ground stations) systems. In Figure 15, the flight profile of the COMAS SOLA balloon is reported as monitored by GPS. The payload landed after a 3-hour flight, at about 200 km from the launch site. Since it landed on a hilly slope, it overturned. The Huygens mock-up, including HASI subsystems, sensors and the data recording

[1] In honour of the Catalan astronomer José Comas Solà who, in 1908, deduced the existence of an atmosphere on Titan from the visual observation of the limb darkening.

Figure 14. Ascending phase of the COMAS SOLA balloon flight. The secondary balloon, which is lifting the probe mock-up, will be released later on, and the payload will continue its ascent dragged by the primary balloon. A damper has been fixed under the mock-up in order to damp the landing.

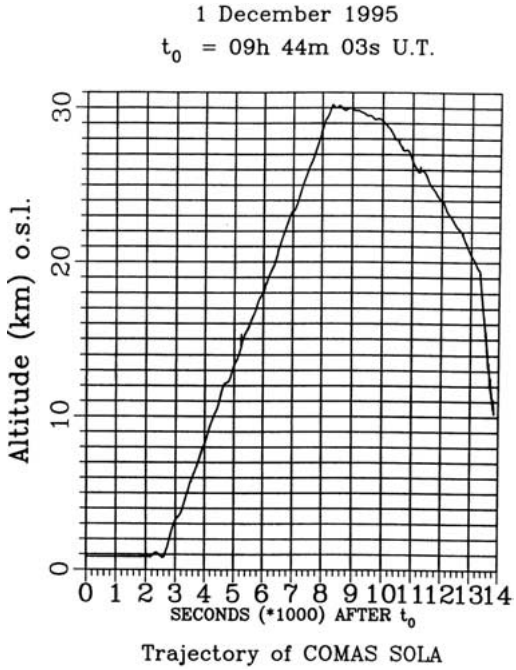

Figure 15. Flight profile of the stratospheric balloon of the COMAS SOLA experiment as derived from GPS data.

and storage systems was recovered in perfect shape with the exception of one of the DBS booms, which was damaged in the probe overturning.

The COMAS SOLA experiment allowed us to take data during the balloon ascent and descent phases in order to check the HASI sensors and the Huygens radar altimeter performance in dynamic and environmental conditions similar to those anticipated during the final part of the Huygens probe descent in Titan's atmosphere. The results obtained represented an in-flight functional test of all the sensors, particularly the PWA, since electric measurements at ground level are strongly affected by the anthropogenic electromagnetic environment. The experiment provided an essential test for the radar altimeter operation, which revealed anomalous instabilities and irregularities in a previous balloon test operated by the Huygens project.

6.1.1. *Temperature Profiles*

The temperature measurements were obtained by the two TEM units mounted on the STUB; an additional PT100 thermistor was positioned as close as possible to TEM1, to be used as reference. Other temperature measurements were taken by the balloon housekeeping sensors and included in the telemetry data. All the sensors measured the atmospheric temperature conditions during the balloon ascending phase and the first part of the descent, corresponding to an altitude range

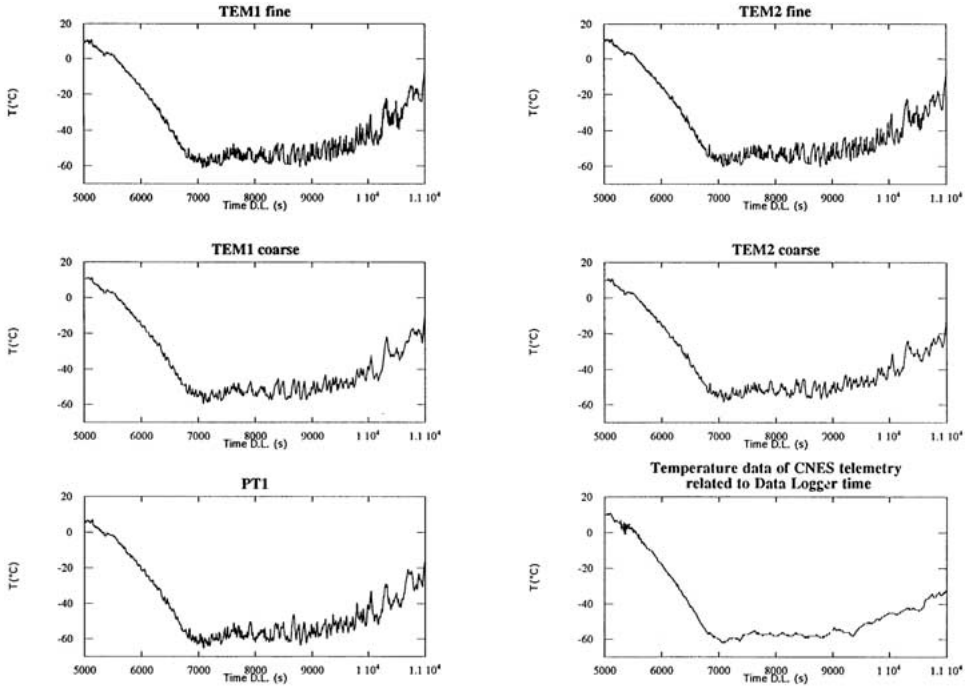

Figure 16. Atmospheric vertical profile recorded between 0.8 and 30 km by the different temperature sensors of the COMAS SOLA experiment. Data are plotted as functions of time as recorded by the data logger used for data recording and storage (5000 s D.L. time = 10:25:39 TU balloon launch).

between 0.8 km and 30 km, with a 1 Hz sampling frequency. Atmospheric temperature profiles obtained from each of the TEM sensors and the PT100 thermistor (PT1) are shown in Figure 16, together with the profile derived from the balloon housekeeping temperature data.

The TEM measurements are more sensitive and are characterised by shorter time constants and better spatial resolution than the PT100: consequently, the TEM sensors recorded wider temperature variations compared to the average value. The profiles derived from the different sensors show a good correlation. From the spectral analysis of the profiles derived from the TEM fine and coarse sensors, we conclude that the dynamic behaviour of the sensors in atmospheric conditions is coherent with the results of the dynamic numerical model (Angrilli *et al.*, 1997). Two major periodicities in the temperature variations have been detected corresponding to altitude scales of about 1400 and 450 m related to atmospheric features.

6.1.2. *Pressure Profiles*

A PPI-based subsystem was used to determine the pressure profile (Mäkinen *et al.*, 1998). The Kiel probe, mounted at the STUB tip, was connected with the capacitive pressure sensors and the temperature sensors located inside the probe, within the electronic box. The pressure measurements combined with the simultaneous tem-

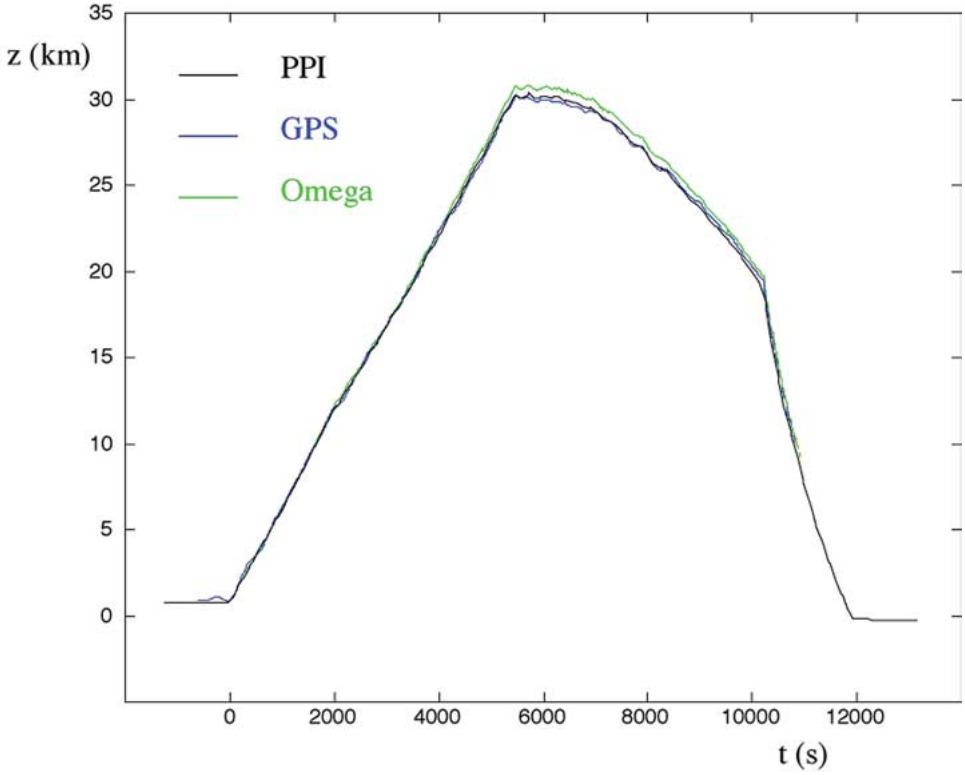

Figure 17. Flight trajectory of the COMAS SOLA experiment. In the plot the trajectory derived from the GPS data and the one computed starting from PPI pressure measurements through the hydrostatic equation are reported. The time in abscissa refers to the initial instant of the balloon launch.

perature measurements permit the reconstruction of the flight vertical trajectory and the pressure profile (Figures 17 and 18). Some turbulent phenomena have been detected.

6.1.3. *Atmospheric Conductivity*

The PWA subsystem was similar to the one included on the Huygens probe, in order to take advantage of the ideal testing conditions represented by the balloon experiment. Measurements of air conductivity, electric fields, and acoustic waves were carried out all along the flight duration, as well as for the processing of the radar echo signal. In the COMAS SOLA experiment, only one radar was used and the booms were fixed on the mock-up ring in deployed configuration.

The relaxation probes mounted on the booms have been used to perform two different measurements: (i) the measure of τ, the relaxation time constant that gives an indication of the ion conductivity in the atmosphere, and (ii) the detection of electric fields, e.g. lightning. In the first case, the relaxation probe electrodes are charged at ± 5 V and then connected to the PWA electrometer, in the second one,

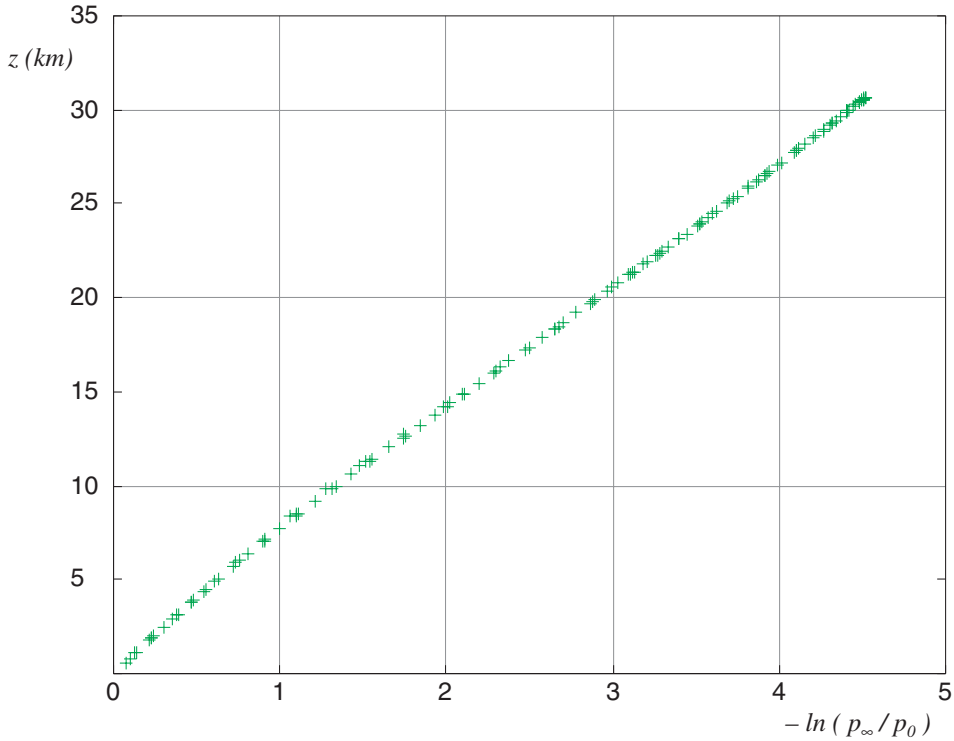

Figure 18. Vertical pressure profile derived from the HASI PPI measurements during the ascending phase of the COMAS SOLA experiment.

the electrodes are connected to ground and the measured tension represents the electric field of the mock-up. Conductivity is obtained by dividing the dielectric constant ε_0 by the relaxation time τ

$$\sigma = \varepsilon_0/\tau(\Omega m)^{-1} \tag{4}$$

The wide range of results for the conductivity of Earth's atmosphere by different experiments in fair weather conditions have been fitted by Rosen & Hofmann (1981) by an empirical formula that gives the conductivity as a function of the pressure

$$\sigma_+ = 3789 P^{-0.6975}\, e^{-0.002899 P} \tag{5}$$

where σ_+ is in $10^{-4}(\Omega\mathrm{m})^{-1}$ and P is the pressure in hPa.

As shown in Figure 19, conductivity at low altitude does not follow the theoretical model (5) and the values obtained during the ascent are different from those obtained during the descent. Conductivity values obtained from the charge decay curves are different at different time intervals and the observed differences depend on the altitude (i.e. the pressure) and vary with positive or negative charging ($\pm$ 5 V). This peculiar behaviour of the relaxation probes during the COMAS

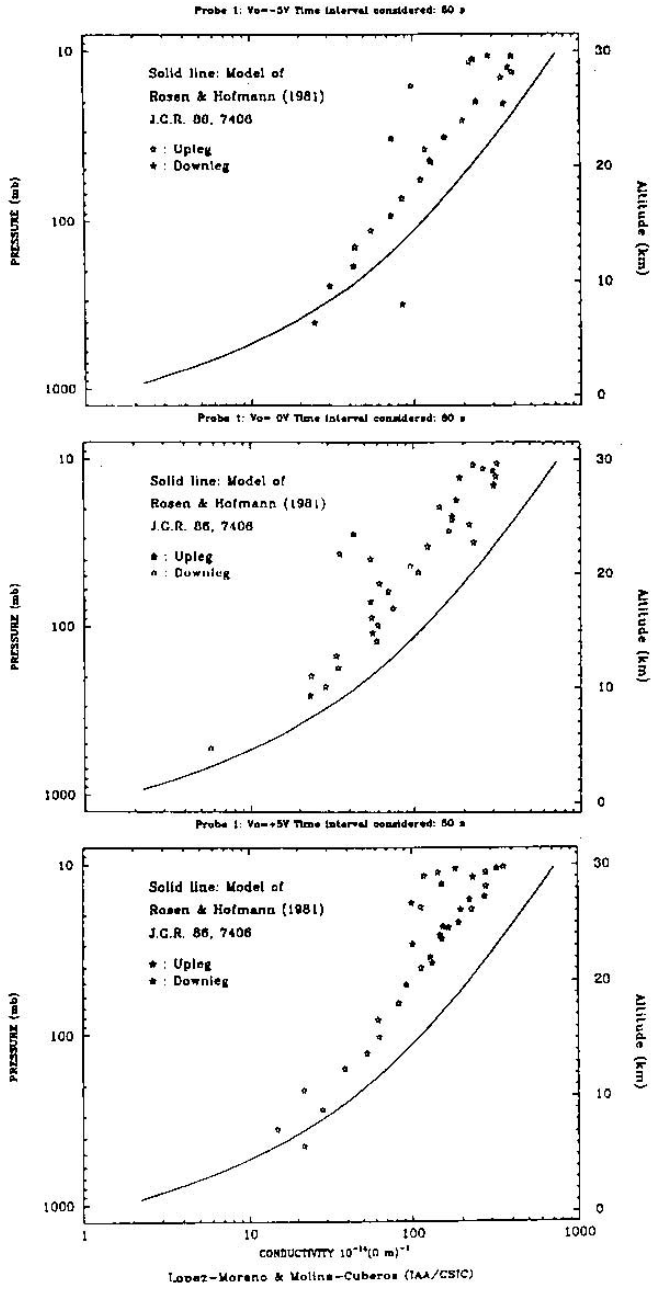

Figure 19. Vertical profiles of atmospheric ion conductivity as derived from one of the PWA relaxation probes during the COMAS SOLA balloon flight. The three profiles have been derived from the discharge curve starting from three different initial states: −5 V, 0 V, +5 V. The conductivity profile (5) (Rosen and Hofmann, 1981) is also reported together with the experimental data.

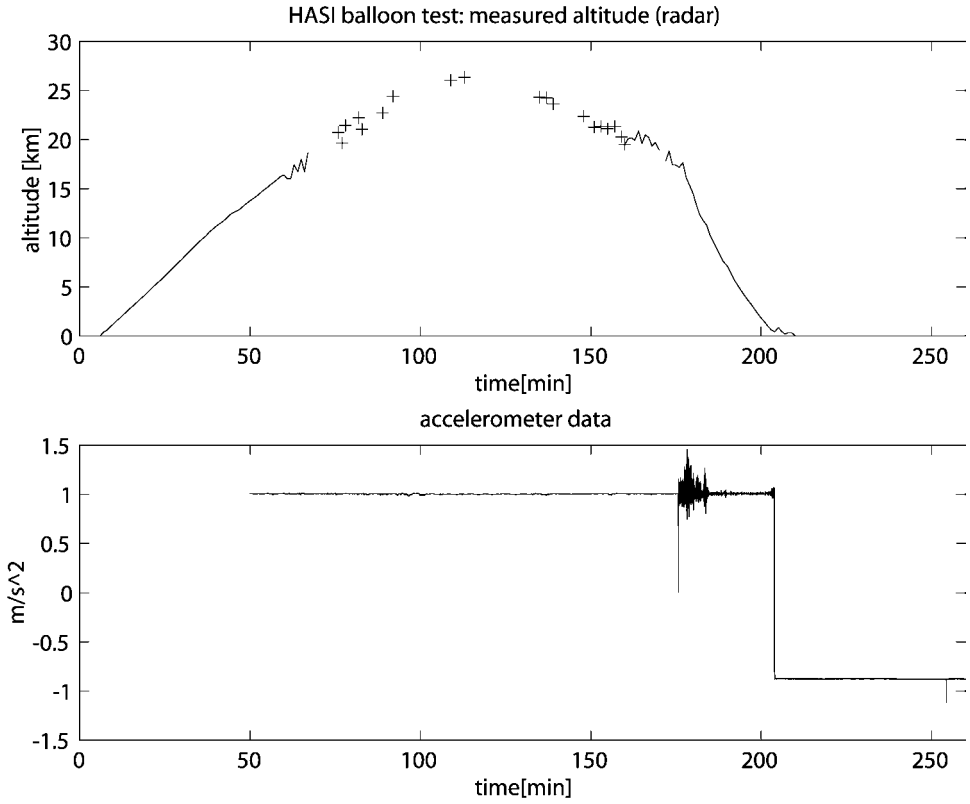

Figure 20. The altitude profile with respect to the ground level as measured by the radar altimeter and the acceleration data as recorded by ACC (in the lower box). On the acceleration measurements are clearly visible the impact trace and the subsequent overturning of the mock-up, which landed on a hill slope.

SOLA experiment is probably due to the distortion of the electric environment caused by balloon electrostatic charging (Grard, 1998).

6.1.4. *Radar Altimetry*

The objectives of the COMAS SOLA experiment for the radar altimeter were to analyse the instabilities and irregularities observed during the previous Huygens balloon drop test, investigate possible solutions, and test and verify the effect of the radar upgrade in realistic conditions. During the COMAS SOLA flight the radar had stability problems. The altimeter behaved nominally up to 16.5 km, but at higher altitudes, even in the presence of a strong return signal, instability in the control cycle produced a noisy blanking signal and losses of lock (see Figure 20). The non-linearity of the sweep ramp strongly limited the resolution for surface topography measurements. Good correspondence was obtained between GPS and radar altitudes.

Analysis of the COMAS SOLA results, combined with those obtained from other radar models, allowed the selection of some solutions and modifications to be implemented on the Huygens proximity sensor in order to optimise its performance. Integration time has been reduced in order to ensure the radar signal lock at higher altitudes, while the control cycle has been modified to achieve stability. A better dynamic synchronisation technique has been used to implement the efficiency of sweep ramp linearity and then to improve the resolution of topography measurements.

6.1.5. *Acceleration Measurements*
ACC was triggered to perform measurements during the descent phase and to detect the surface impact trace. This part of the balloon flight is the most representative of the Huygens mission at Titan and provided the opportunity to test the accelerometer performance and measurement cycle, especially the impact detection under real conditions. The accelerometer correctly detected the impact with the terrestrial surface and recorded the subsequent overturning of the mock-up.

7. First HASI Data from Space

During the Cassini cruise phase the Huygens probe is in sleep mode. Periodically, it is switched on to perform a health check. The probe, its subsystems and the experiments are tested in a mission simulation sequence in order to verify the health status. Eight days after launch, the Huygens probe was switched on for the first time and performed the first in-flight checkout successfully. Then, about every six months the probe is switched on and checked until the Saturn insertion orbit.

During the first in-flight checkouts, the HASI behaviour was nominal. The HASI sensors appear to be functioning within their nominal parameter range; the measurements are normal and consistent with the expected space environmental conditions. The ambient spacecraft acceleration conditions were outside the sensitive range of ACC sensors. The acceleration values sensed when ACC was set in the high-resolution range are of the order of 20 μg (the sensor offset at 0 g). ACC did not record any effects due to Cassini thruster activations for three-axes-stabilised spacecraft attitude control. The PPI pressure sensor readings were approximately 0 hPa and the constant capacitor readings close to nominal values, as expected in deep space vacuum conditions.

8. Conclusions

The HASI experiment is on its way to Titan. The in-flight health checks of the Huygens probe show that our instrument is in a very good shape. The success of prior atmospheric structure experiments (e.g., Pioneer Venus and Galileo ASI)

in achieving similar goals at other planetary bodies, reinforces the feasibility of HASI goals for Titan's investigation. We are preparing the mission at Titan in order to maximise the scientific output, exploiting the results of new observations, theoretical and experimental models (new balloon flights, numerical modelling, laboratory simulations).

Acknowledgements

The authors wish to acknowledge F. Boldrini, V. G. Brown, A. Buccheri, M. Chabassier, C. Cornaro, M. Cosi, R. De Vidi, S. Debei, G. Fanti, B. Hathi, I. Jernej, J. M. Jeronimo, H. Jolly, A. Lehto, T. Mäkinen, B. Saggin for their contribution to the HASI experiment.

References

Angrilli, F., Bianchini, G., Debei, S., Fanti, G., Ferri, F., Fulchignoni, M., and Saggin, B.: 1996, 'First results of performance test of temperature sensors of HASI instrument on Huygens-Cassini mission', *Proceedings SPIE Denver 5–6 August 1996*, **2803-09**, 75–83.

Angrilli, F., Bianchini, G., Da Forno, R., Debei, S., Fanti, G., Ferri, F., and Saggin, B.: 1997, 'Performance verification of a resistance thermometer for atmospheric measurements', in the proceedings of *TEMPMEKO'96 6th International Symposium on Temperature and Thermal Measurements in Industry and Science*, Torino, Italy, September 1996, Piero Macarino, eds., Torino, Italy, Levrotto & Bella, 163–167.

Bird, M. K., Dutta-Roy, R., Heyl, M., Allison, M., Asmar, S. W., Folkner, W. M., Preston, R. A., Atkinson, D. H., Edenhofer, P., Plettemeier, D., Wohlmuth, R., Iess, L. and Tyler, G. L.: 2002, 'The Huygens Doppler Wind Experiment', *Space Sci. Rev.*, **104**, 613–640.

Borucki, W. J., McKay, C. P., and Whitten, R. C.: 1984, 'Possible production by lightning of aerosols and trace gases in Titan's atmosphere', *Icarus*, **60**, 260.

Borucki, W. J., Levin, Z., Whitten, R. C., Keesee, R. G., Capone, L. A., Summers, A. L., Toon, O. B., and Dubach, J.: 1987, 'Predictions of the electrical conductivity and charging of the aerosols in Titan's atmosphere', *Icarus*, **76**, 125.

Courtin, R., Gautier, D., and McKay, C. P.: 1995, 'Titan's thermal emission spectrum: Re-analysis of the Voyager infrared measurements', *Icarus*, **114**, 144–162.

Coustenis, A., Bézard, B., and Gautier, D.: 1989, 'Titan's atmosphere from Voyager infrared observations: I The gas composition of Titan's equatorial region', *Icarus*, **80**, 54–76.

Coustenis, A., Bézard, B., Gautier, D., Marten, R. A., and Samuelson, R.: 1991, 'Titan's Atmosphere from Voyager infrared observations: III Vertical distribution of hydrocarbons and nitriles near Titan's North Pole', *Icarus*, **89**, 152–167.

Coustenis, A. and Bézard, B.: 1995a, 'Titan's atmosphere from Voyager Infrared Observations: IV Latitudinal variations of temperature and composition', *Icarus*, **115**, 126–140.

Coustenis, A., Lellouch, E., Maillard, J. P., and McKay, C. P.: 1995b, 'Titan surface: composition and variability from the near infrared albedo', *Icarus*, **118**, 87–104.

Desch, M. D. and Kaiser, M. L.: 1990, 'Upper limit set for the level of lightning activity on Titan', *Nature*, **242**, 442–443.

Flasar, F. M., Samuelson, R. E. and Conrath, B. J.: 1981, 'Titan's atmosphere: temperature and dynamics', *Nature*, **292**, 693–698.

Fulchignoni, M.: 1992, 'The atmosphere of Titan and the Huygens Atmospheric Structure Instrument', *Il nuovo cimento*, **15C**, 1163–1177.

Fulchignoni, M., Angrilli, F., Bianchini, G., Bar-Nun, A., Barucci, M. A., Borucki, W., Coradini, M., Coustenis, A., Ferri, F., Grard, R., Hamelin, M., Harri, A. M., Leppelmeier, G. W., Lopez-Moreno, J. .J., McDonnell, J. A. M., McKay, C., Neubauer, F. H., Pedersen, A., Picardi, G., Pirronello, V., Pirjola, R., Rodrigo, R., Schwingenschuh, K., Seiff, A., Svedhem, H., Thrane, E., Vanzani, V., Visconti, G., and Zarnecki, J.: 1997, 'The Huygens Atmospheric Structure Instrument (HASI)', in *Huygens Science, Payload and Mission*, **ESA-SP-1177**, 163–176.

Grard, R., Svedhem, H., Brown, V., Falkner, P., and Hamelin, M.: 1995, 'An experimental investigation of atmospheric electricity and lightning activity to be performed during the descent of the Huygens probe onto Titan', *J. Atmos. Terr. Phys.*, **57**, 575.

Grard, R.: 1997, 'Atmospheric electricity and lighting activity models for Titan', in *Huygens Science, Payload and Mission*, **ESA SP-1177**, 257–263.

Grard, R.: 1998, 'Electrostatic charging processes of balloon and gondola surfaces in the Earth atmosphere', *J. Geophys. Res.*, **103**, 23 315–23 320.

Griffith, C. A., Owen, T., and Wagener, R.: 1991, 'Titan's surface and troposphere investigated with ground-based, near-infrared observations', *Icarus*, **93**, 362–368.

Harri, A.-M, Fagerström, B., Lehto, A., Leppelmeier, G. W., Mäkinen, T., Pirjola, R., Siikonen, T., and Siili, T.: 1998, 'Scientific objectives and implementation of the Pressure Profile Instrument (PPI/HASI) for the Huygens spacecraft', *Planet. Space Sci.*, **46/9-10**, 1383–1392.

Hubbard, W. B., Siacrdy, B., Miles, R., Hollis, A. J., Forrest, R. W., Nicolson, I. K. M., Appley, G., Beisker, W., Bittner, C., Bode, H. J., Bruns, M., Denzau, H., Nezel, M., Rieldel, E., Struckmann, H., Arlot, J. E., Roques, F. Sevre, F., Thuillot, W., Hoffman, M., Geyer, E. H., Buil, C., Colas, F., Lecacheux, J., Klotz, A., Thouvenot, E., Vidal, J. L., Carreira, E., Rossi, F., Blanco, C., Cristaldi, S., Nevo, Y., Reisema, H. J., Brosch, N., Cernis, K., Zdanavicius, K., Wasserman, L. H., Hunten, D. M., Gautier, D., Lellouch, E., Yelle, R. V., Rizk, B., Flasar, F. M., Porco, C. C., Toublanc, D., and Corugendo, G.: 1993, 'The occultation of 28 Sgr by Titan', *Astronomy and Astrophysics*, **269**, 541–564.

Hunten, D. M., Tomasko, M. G., Flasar, F. M., Samuelson, R., Strobel, D. F., and Stevenson, D. J.: 1984, 'Titan' in *Saturn*, T.Gehrels and M.S. Matthews, Eds., Tucson, The University of Arizona Press, 671–759.

Ip, W.-H.: 1990, 'Titan's upper armosphere', *Astrophys. J.* **362**, 354–363.

Israel, G., Cabane, M., Brun, J.-F., Niemann, H., Way, S., Riedler, W., Steller, M., Raulin, F., and Coscia, D.: 2002, 'Huygens Probe Aerosol Collector Pyrolyser Experiment', *Space Sci. Rev.* **104**, 433–468.

Lara, L. M., Lorenz, R. D., and Rodrigo, R.: 1994, 'Liquid and solid on the surface of Titan: Result of a new photochemical model', *Planet. Space. Sci.*, **42**, 5–14.

Lara, L. M., Lellouch, E., López-Moreno, J. .J. and Rodrigo, R.: 1996, 'Vertical distribution Titan's atmospheric neutral constituents', *J. Geophys. Res.* **101**, 23 261–23 283, (corrections in **103**, 25 775, 1998).

Lellouch, E., Hunten, D., Kockarts, G., and Coustenis, A.: 1990, 'Titan's thermosphere profile', *Icarus* **83**, 308–324.

Lemmon, M. T., Karkoschka, E., and Tomasko, M.: 1995, 'Titan's rotation light curve', *Icarus*, **113**, 27–38.

Lindal, G. F., Wood, G. E., Hotz, H. B., and Sweetnam, D. N.: 1983, 'The atmosphere of Titan: an analysis of Voyager 1 radio occultation measurement', *Icarus*, **53**, 348–363.

Lorenz, R. D.: 1993, 'The life, death and after life of a raindrop on Titan', *Planet. Space Sci.* **41**, 647.

Lunine, J. I., Stevenson, D. J., and Yung, Y. L.: 1983, 'Ethane ocean on Titan', *Science*, **222**, 1229–1230.

Lunine, J. I. and Lorenz, R. D.: 1996, 'Surface of Titan revealed by Cassini/Huygens', in *Proceedings SPIE* Denver 5–6 August 1996, **2803-06**, 45–54.

Mäkinen, T., Salminen, P., Lehto, A., Leppelmeier, G., and Harri, A.-M.: 1998, 'PPI results from the balloon drop experiment of the HASI pressure profile instrument', *Planet. Space Sci.*, **46/9-10**, 1237–1243.

McKay, C. P., Pollack, J. B., and Courtin, R.: 1989, 'The thermal structure of Titan's atmosphere', *Icarus*, **80**, 23–53.

McKay, C. P., Martin, S. C., Griffith, C. A., and Keller, R. M.: 1997, 'Temperature lapse rate and methane in Titan's troposphere', *Icarus*, **129**, 498–505.

Muhleman, D. O., Grossman, A. W., and Butler, B. J.: 1995, 'Radar investigation of Mars, Mercury, and Titan', *Ann. Rev. Earth and Planet. Sci.* **23**, 337–374.

Navarro-Gonzales R., and Ramirez, S. I.: 1997, 'Corona discharge of Titan's troposphere', *Adv. Space Res.*, **19**, 1121–1133.

Niemann, H. B., Atreya, S. K., Bauer, S. J., Biemann, K., Block, B., Carignan, G. R., Donahue, T. M., Frost, R. L., Gautier, D., Haberman, J. A., Harpold, D., Hunten, D. M., Israel, G., Lunine, J. I., Mauersberger, K., Owen, T. C., Raulin, F., Richards, J. E., and Way, S. H.: 2002, 'The Gas Chromatograph Mass Spectrometer for the Huygens Probe', *Space Sci. Rev.*, **104**, 553–591..

Polk, C.: 1982, 'Schumann Resonances' in *Handbook of Atmospherics*, Ed. H. Volland, Boca Raton, Florida, USA, CRC Press, 111–178.

Rinnert, K.: 1985, 'Lightning on other planets', *J. Geophys. Res.*, **90**, 6225–6237.

Rosen, J. L. M. and Hofmann, D. J.: 1981, 'Balloon-borne measurements of electrical conductivity, mobility and recombination coefficient', *J. Geophys. Res.*, **86**, 7406–7410.

Ruffino, G., Castelli, A., Coppa, P., Cornaro, C., Foglietta, S., Fulchignoni, M., Gori, F., and Salvini, P.: 1996, 'The temperature sensor on the Huygens probe for the Cassini mission: Design, manufacture, calibration and tests of the laboratory prototype', *Planet. Space Sci.*, **44-10**, 1149–1162.

Sagan C. and Thompson, W. R.: 1984, 'Production and condensation of organic gases in the atmosphere of Titan', *Icarus*, **59**, 133–161.

Schofield, J. T., Barnes, J. R., Crisp, D., Haberle, R. M., Larsen, S., Magalhaes, J. A., Murphy, J. R., Seiff, A. and Wilson, G.: 1997, 'The Mars Pathfinder Atmospheric Structure Investigation/Meteorology (ASI/MET) Experiment', *Science*, **278**, 1752–1758.

Seiff, A., Kirk, D. B., Young, R. E., Blanchard, R. C., Findlay, J. T., Kelly, G. M., and Sommer, C.: 1980, 'Measurements of thermal structure and thermal contrast in the atmosphere of Venus and related dynamical observations: Results from the four Pioneer Venus probes', *J. Geophys. Res.*, **85**, 7903–7933.

Seiff, A.: 1993, 'Mars atmospheric winds indicated by motion of the Viking landers during parachute descent', *J. Geophys. Res.*, **98**, 7461–7474.

Seiff, A., Blanchard, R. C., Knight, T. C. D., Schubert, G., Kirk, D. B., Atkinson, D., Mihalov, J. D., and Young, R. E.: 1997a, 'Wind speed measured in the deep Jovian atmosphere by the Galileo probe accelerometer', *Nature*, **388**, 650–652.

Seiff, A., Tillmann, J. E., Murphy, J. R., Schofield, J. T., Crisp, D., Barnes, J. R., LaBaw, C., Mahoney, C., Mihalov, J. D., Wilson, G. R., and Haberle, R.: 1997b, 'The atmosphere structure and meteorology instrument on the Mars Pathfinder lander', *J. Geophys. Res.*, **102**, 4045–4056.

Seiff, A., Kirk, D. B., Knight, T. C. D., Young, R. E., Mihalov, J. D., Young, L., Milos, F. S., Schubert, G., Blanchard, R. C., and Atkinson, D.: 1998, 'Thermal structure of Jupiter's atmosphere near the edge of a 5 μm hot spot in the north equatorial belt', *J. Geophys. Res.*, **103**, 22 857–22 889.

Sicardy, B., Ferri, F., Roques, F., Brosh, N., Nevo, Y., Hubbard, W. B., Reitsema, H. R., Blanco, C., Cristaldi, S., Carreira, E., Rossi, F., Lecacheux, J., Pau, S., Beisker, W., Bittner, C., Bode, H.-J., Bruns, M., Denzau, H., Nezel, M., Riedel, E., Struckmann, H., Appleby, G., Forrrest, R. W., Nicolson, I. K. M., Miles, R., and Hollis, A. J.: 1999, 'The structure of Titan's stratosphere from the 28 Sgr occultation', *Icarus*, **142**, 357–390.

Smith, P. H., Lorenz, R. D., and Lemmon, M. T.: 1995, 'New information on Titan's north-south contrast from HST', *Bull. Am. Astron. Soc.*, **27**, 1104.

Smith, P. H., Lemmon, M. T., Lorenz, R. D., Sromovsky, L. A., Caldwell, J. J., and Allison, M. D.: 1996, 'Titan's surface revealed by HST imaging', *Icarus*, **119**, 336–349.

Strobel, D. F. and Sicardy, B.: 1997, 'Gravity wave and wind shear models', in *Huygens Science, Payload and Mission*, **ESA-SP-1177**, 299–312.

Tomasko, M. G., Buchhauser, D., Bushroe, M., Dafoe, L. E., Doose, L. R., Eibl, A., Fellows, C., McFarlane, E., Prout, G. M., Pringle, M. J., Rizk, B., See, C., Smith, P. H., and Tsetsenekos, K.: 2002, 'The Descent Imager/Spectral Radiometer (DISR) Experiment on the Huygens Entry Probe of Titan', *Space Sci. Rev.*, **104**, 469–551.

Toon, O. B., McKay, C. P., Courtin, R., and Ackerman, T. P.: 1988, 'Methane rain on Titan', *Icarus*, **75**, 255–284.

Yelle, R.: 1991, 'Non-LTE models of Titan's upper atmosphere', *Astrophys. J.*, **383**, 380–400.

Zarnecki, J. C., Leese, M. R., Ghafoor, J. R. C., and Hathi, B.: 2002, 'Huygens' Surface Science Package', *Space Sci. Rev.*, **104**, 593–611.